

The 9<sup>th</sup> Conference  
on Functional and Nanostructured Materials

**FNMA'12**

23–27 September 2012  
Egina Island, Greece

**ABSTRACT BOOK**

TITLE

*The 9<sup>th</sup> Conference on Functional and Nanostructured Materials – FNMA'12*  
*23–27 September 2012, Egina, Greece – Abstract Book*

EDITORS

*Jarosław Rybicki and Krzysztof W. Wojciechowski*

TYPESETTING USING T<sub>E</sub>X

*BOP s.c., [www.bop.com.pl](http://www.bop.com.pl)*

TASK PUBLISHING 2012  
GDAŃSK

ISBN 978-83-930549-7-8

FNMA'12 –  
THE 9<sup>th</sup> CONFERENCE ON FUNCTIONAL  
AND NANOSTRUCTURED MATERIALS

ORGANIZERS

Department of Solid State Physics, Faculty of Physics,  
University of Athens, Greece

Department of Solid State Physics, Gdansk University of Technology, Poland  
Institute of Physics, Faculty of Mechanical Engineering and Mechatronic,  
West Pomeranian University of Technology, Szczecin, Poland

Institute of Molecular Physics, Polish Academy of Sciences, Poznan, Poland  
PWSZ im. Prezydenta St. Wojciechowskiego, Kalisz, Poland  
Institute of Physics, University of Zielona Gora, Poland

IN COOPERATION WITH:

TASK – Academic Computer Centre in Gdansk, Poland  
Poznan Supercomputing and Networking Center, Poland  
Intel Corporation      Polish Physical Society

HONORARY CHAIRMAN

G. J. Papadopoulos, (Athens, Greece)

SCIENTIFIC COMMITTEE

- A. Alderson (Bristol, UK) • K. L. Alderson (Bristol, UK) • F. J. Baltá-Calleja (Madrid, Spain)  
J. Barnaś (Poznan, Poland) • J. Bernholc (Raleigh, USA) • X. M. Duan  
(Beijing, China) • A. C. Griffin (Atlanta, USA) • J. Grima (Msida, Malta)
- B. Grzybowski (Evanston, USA) • W. G. Hoover (Ruby Valley, USA) • A. B. Kolomeisky  
(Houston, USA) • A. A. Kornyshev (London, UK) • H. Mizuta (Southampton, UK)
- A. Morawski (Szczecin, Poland) • G. Papavasiliou (Athens, Greece) • V. Radmilovic  
(Berkeley, USA) • P. Siskos (Athens, Greece) • W. Sadowski (Gdansk, Poland) –  
Co-Chairman • F. Scarpa (Bristol, UK) • K. Schulte (Hamburg, Germany)
- T. Tsuboi (Kyoto, Japan) • P. Varotzos (Athens, Greece) • K. W. Wojciechowski  
(Poznan, Poland) – Co-Chairman • N. I. Zheludev (Southampton, UK)

PROGRAMME COMMITTEE

- M. Dudek (Zielona Gora, Poland) • N. Gouskos (Athens, Greece) • R. Gunnella (Camerino, Italy)  
S. Kruchinin (Kiev, Ukraine) • J. Olchowik (Lublin, Poland) • U. Narkiewicz (Szczecin,  
Poland) • B. Padlyak (Lviv, Ukraine) • D. Petridis (Athens, Greece) – Co-Chairman • J. Rybicki  
(Gdansk, Poland) – Co-Chairman • Ch. Trapalis (Athens, Greece) • J. Typek (Szczecin, Poland)

ORGANIZING COMMITTEE

- N. Guskos, University of Athens – Chairman • C. Aidinis, University of Athens  
I. Chadziagapiou, University of Athens • K. Karkas, University  
of Athens • V. Likodimos, University of Athens • A. Malakis, University of Athens  
M. Nakonieczny (Gdansk, Poland) • D. Petridis, Demokritos, Athens • J. Rybicki  
(Gdansk, Poland) • N. Sarlis, University of Athens • A. Spanopoulou, University  
of Athens • Ch. Trapalis, Dimokritos, Athens • B. Zapotoczny (Zielona Gora, Poland)

# CONTENTS

## LECTURES

J. F. Annett, <u>S. P. Kruchinin</u> , A. A. Zolotovskiy <i>Andreev billiard states of hybrid superconducting nanowires</i> .....	13
F. J. Baltá-Calleja, F. Ania, A. Flores <i>Nanostructure characterization of multilayered polymers using synchrotron radiation techniques: crystallization phenomena</i> .....	14
V. Belomestnykh, <u>E. Soboleva</u> <i>Poisson's ratios of <math>Cu_2O</math> crystals under temperature changes</i> .....	16
<u>Z. Czech</u> , A. Butwin, D. Sowa <i>Solvent-based acrylic pressure-sensitive adhesives crosslinked using UV-radiation</i> .....	18
<u>X.-M. Duan</u> <i>Microstructures of functional polymer nanocomposites fabricated by two-photon photopolymerization</i> .....	19
<u>Z. Gburski</u> , K. Górny, P. Raczyński, M. Pabiszczak <i>Influence of graphene on cholesterol lodgment localized on protein surface – computer simulation study</i> .....	21
<u>D. Gournis</u> <i>Novel synthetic approaches for development of two-dimensional hybrid functional materials</i> .....	22
N. Gouskos, A. Guskos, G. Żołnierkiewicz, J. Typek, P. Berczyński, D. Dolat, B. Grzmil, <u>A. Morawski</u> <i>EPR study of annealing and rinsing of <math>TiO_2</math> nanocrystalline materials</i> .....	23
<u>N. Gouskos</u> , G. Żołnierkiewicz, A. Guskos, J. Typek, J. Borucka-Lipska, W. Kiernożycki <i>EPR/FMR studies of cement slurry with different magnetite concentration</i> .....	24

<u>J. N. Grima, R. Gatt, D. Attard, L. Mizzi, J. D. Cutajar, A. Casha, R. Cauchi, Ch. Zerafa, R. Caruana-Gauci, B. Ellul, M. Camilleri, E. Manicaro, E. Chetcuti</u> <i>On the effect of imperfections on the Poisson's ratios and other properties of crystalline and cellular systems with particular reference to their auxetic potential</i> .....	25
<u>M. Grinberg</u> <i>High pressure study of localized states related to <math>Ln^{3+}</math> and <math>Ln^{2+}</math> ions in solids</i> .....	26
<u>I. Hadjiagapiou</u> <i>Three-dimensional Ising model with fluctuating exchange integral in asymmetric bimodal random field: effective field theory – differential operator technique</i> .....	27
<u>T. A. M. Hewage, K. L. Alderson, A. Alderson</u> <i>A 2-constituent system displaying negative effective Poisson's ratio and negative effective stiffness</i> .....	28
<u>A. R. Imre</u> <i>Possible auxeticity in some natural solid/liquid systems</i> .....	29
<u>J. Kaszewski, S. Yatsunenko, M. Godlewski, I. Pełech, P. Łukaszczyk, E. Mijowska, G. Żołnierkiewicz, N. Gouskos, E. Kusiak, J. Orlikowski, W. Morawski, U. Narkiewicz</u> <i>Structural and luminescent properties of microwave hydrothermal synthesized <math>ZrO_2</math> nanopowders</i> .....	30
<u>W. Kempieński, M. Kempieński, D. Markowski, Sz. Łoś</u> <i>Localization of carriers and spins in nanocarbons</i> .....	32
<u>K. Kwiatkowski, M. Kwiatkowska</u> <i>Multiphase reactive blends based on thermoplastic polyester</i> .....	33
<u>W. Nawrocki</u> <i>Towards quantum limits in scaling of electronic devices</i> .....	35
<u>B. V. Padlyak, A. V. Kopayev, Yu. N. Tafiychuk, D. L. Zadnieprianni, A. Drzewiecki</u> <i>Structure, magnetic properties and FMR spectroscopy of Ni-Al nanoferrites</i> .....	39
<u>G. J. Papadopoulos</u> <i>Real time quantum tunneling</i> .....	41

<u>D. Petridis, E. C. Vermisoglou, N. Todorova, T. Giannakopoulou, N. Gouskos, C. Trapalis</u> <i>Pillaring of GO by stabilized cationic benzidine free radicals</i> .....	42
<u>P. Polanowski</u> <i>Cooperative dynamics in frame of a dynamic lattice liquid (DLL) model as a tool to simple and complex liquids simulations</i> .....	43
<u>F. X. Qin, H. X. Peng</u> <i>Amorphous and nanocrystalline ferromagnetic microwires enabled multifunctional composites</i> .....	44
<u>W. Ren, P. J. McMullan, W. Kline, A. C. Griffin</u> <i>Nanoscale origins of thermally-driven strain recovery in some shape-memory liquid crystalline networks</i> .....	46
<u>N. V. Sarlis</u> <i>Similarity of fluctuations of critical systems in natural time</i> .....	47
<u>A. Sikorski, S. Jaworski, Ł. Ołdziejewski</u> <i>Dynamics of polymer chains near a patterned surface in a slit and in a tube – a computer simulation study</i> .....	49
<u>N. Todorova, E. C. Vermisoglou, M. Giannouri, T. Giannakopoulou, D. Petridis, C. Trapalis</u> <i>Graphite to graphene oxide conversion and decoration with silver nanoparticles using solar light</i> .....	50
<u>J. Typek, N. Gouskos, K. Wardal, G. Żolnierkiewicz</u> <i>Comparison of magnetic characterizations of nanoparticles obtained by SQUID magnetometry and FMR</i> .....	51
<u>K. W. Wojciechowski, A. A. Poźniak</u> <i>Materials of anomalous mechanical properties</i> .....	52
<u>B. Zapotoczny, M. R. Dudek, N. Gouskos, J. J. Koziół, B. V. Padlyak, E. Rysiakiewicz-Pasek</u> <i>Filling porous silicate glasses with <math>Fe_3O_4</math> magnetic nanoparticles</i> .....	53
<u>P. Zygori, P. Stathi, T. Tsoufis, A. Kouloumpis, D. Gournis, P. Rudolf</u> <i>A modified Langmuir-Schaefer approach to synthesis of highly-ordered clay/carbon nanotube hybrids</i> .....	55

## POSTERS

<u>A. Amirabadizadeh</u> <i>Comparative study of methods for synthesizing mixed nanoferrites and of their magnetic properties</i> .....	59
--	----

<u>M. Białoskórski, J. Rybicki</u> <i>Nanomechanical properties of metallic fcc nanorods from molecular simulations with the Sutton-Chen force field</i> .....	60
<u>E. Bletsa, Y. Deligiannakis, D. Gournis</u> <i>Long-lasting solubilisation of multi-walled carbon nanotubes by synthetic humic acids</i> .....	62
<u>R. Caruana-Gauci, M. R. Dudek, K. W. Wojciechowski, J. N. Grima</u> <i>Anomalous mechanical behaviour from metamaterials with magnetic components</i> .....	63
<u>R. Caruana-Gauci, K. W. Wojciechowski, J. N. Grima</u> <i>On obtaining negative linear compressibility through elongation of the ribs</i> .....	64
<u>R. Cauchi, K. M. Azzopardi, R. Gatt, D. Attard, J. Rybicki, J. N. Grima</u> <i>Modelling of auxetic crystals</i> .....	66
<u>A. Dawid, K. Górny, Z. Gburski</u> <i>Dynamics of NO molecules near wall of fullerenols <math>C_{60}(OH)_{24}</math> in aqueous solution – MD study</i> .....	67
<u>Z. Dendzik, K. Górny, Z. Gburski</u> <i>Non-Debye dipolar relaxation of ethylene glycol embedded in ZSM-5 zeolite host matrix – computer simulation study</i> .....	69
<u>R. V. Goldstein, V. A. Gorodtsov, D. S. Lisovenko</u> <i>Hexagonal auxetics</i> .....	70
<u>N. Gouskos, S. Glenis, G. Żołnierkiewicz, J. Typek, P. Berczyński, A. Guskos, K. Wardal, D. Sibera, U. Narkiewicz, Z. Lenzion-Bieluń, W. Łojkowski</u> <i>Study of magnetic properties of <math>ZnFe_2O_4</math> nanoparticles at different concentrations of FeO in ZnO matrix</i> .....	73
<u>N. Gouskos, A. Krupska, J. Typek</u> <i>Pressure study of FMR spectra of 0.1% Ni and 0.1% <math>\gamma</math>-<math>Fe_2O_3</math> nanoparticles in copolymer matrix at room temperature</i> .....	74
<u>N. Gouskos, J. Majszczyk, J. Typek, A. Guskos, J. Rybicki</u> <i>Photoacoustic response of red fruit <i>Pyracantha Coccinea</i></i> .....	76
<u>N. Gouskos, D. Petridis, S. Glenis, A. Guskos, P. Berczyński</u> <i>Magnetic properties of composites of <math>\gamma</math>-<math>Fe_2O_3</math> nanoparticles covered by <math>Me_3[Fe(CN)_6]_2 \cdot H_2O</math> (<math>Me(II) = Co(II)</math> and <math>Ni(II)</math>)</i> .....	77
<u>N. Gouskos, G. Żołnierkiewicz, J. Typek, D. Sibera, U. Narkiewicz</u> <i>Temperature dependence study of EPR/FMR spectra of nanocrystalline <math>n MnO/(1 - n) ZnO</math> (<math>n = 0.20, 0.30, 0.40</math>)</i> .....	79

<u>J. N. Grima, A. Casha, R. Gatt, K. Dudek, W. Wolak, D. Attard</u> <i>Modelling of auxetic biomedical devices</i> .....	80
<u>P. Kajak, J. Rybicki</u> <i>Melting phenomena in platinum nanoclusters</i> .....	81
<u>P. Kędziora</u> <i>The pretransitional fluctuations in liquid crystalline materials studied by nonlinear dielectric spectroscopy</i> .....	82
<u>B. Kościelska, A. Witkowska, L. Wicikowski</u> <i>Structural investigations of nitrated VN-SiO<sub>2</sub> sol-gel derived films</i> .....	83
<u>S. P. Kruchinin, A. A. Zolotovskiy</u> <i>Optical properties of ceramic nanoparticles</i> .....	84
<u>M. Kwiatkowska, K. Kwiatkowski</u> <i>Crystallization kinetics of multiphase reactive blends in the presence of nanostructured additives</i> .....	85
<u>I. E. Lipiński, M. Soboń</u> <i>Ferromagnetic resonance study of carbon coated nickel and cobalt nanoparticles</i> .....	86
<u>M. Łapiński, A. Bojarska, B. Kościelska, W. Sadowski</u> <i>Structural investigations of lithium titanate spinel oxide nanopowder prepared by low temperature method</i> .....	87
<u>J. W. Narojczyk, M. Kowalik, K. W. Wojciechowski</u> <i>Partially auxetic behavior in fcc crystals of soft polydisperse dimers</i> .....	88
<u>B. V. Padlyak, A. Drzewiecki, S. I. Mudry, Yu. O. Kulyk</u> <i>Structure and spectroscopic properties of undoped borate glasses</i> .....	90
<u>B. V. Padlyak, W. Ryba-Romanowski, R. Lisiecki, N. Gouskos, G. Żolnierkiewicz</u> <i>Optical and EPR spectroscopy of Li<sub>2</sub>B<sub>4</sub>O<sub>7</sub>:Er glasses</i> .....	91
<u>A. A. Poźniak, K. W. Wojciechowski</u> <i>Negative mechanical compliance of constrained auxetic materials</i> .....	93
<u>P. Raczyński, M. Pabiszczak, Z. Gburski</u> <i>Impact of carbon nanotube on homocysteine clusters – MD simulation</i> .....	94
<u>K. V. Tretiakov, K. W. Wojciechowski</u> <i>Poisson's ratio of polydisperse hard disks and spheres</i> .....	95

S. Winczewski, J. Rybicki <i>Structure of small platinum clusters</i> .....	97
A. Witkowska, S. Dsoke, R. Marassi, A. Di Cicco <i>Platinum nano-particles embedded in acidic cesium or rubidium salt matrices: an XAS study</i> .....	98
Ch. Zerafa, M. R. Dudek, A. C. Griffin, K. W. Wojciechowski, J. N. Grima <i>Modelling of liquid crystalline polymers with anomalous mechanical properties</i> .....	100
G. Żołnierkiewicz, N. Gouskos, J. Typek, A. Hełminiak, W. Arabczyk <i>FMR study of influence of nitriding process of promoted nanocrystalline iron and nitrides reduction process at various nitriding potentials</i> .....	103
Personalia <i>The 55<sup>th</sup> birthday of Sergei Kruchinin</i> .....	105
<i>Index of authors</i> .....	108



# LECTURES



# Andreev billiard states of hybrid superconducting nanowires

J. F. Annett<sup>1</sup>, S. P. Kruchinin<sup>2</sup>, A. A. Zolotovskiy<sup>2</sup>

<sup>1</sup>*HH Wills Physics Laboratory, University of Bristol  
Tyndall Avenue, Bristol BS8 1TL, UK*

<sup>2</sup>*Bogoliubov Institute for Theoretical Physics, NASU  
Metrologichna 14b, 03-680 Kiev-143, Ukraine*

High-quality superconducting hybrid nanowires were fabricated using recent technology and experiments. We studied hybrid nanowires in which normal and superconducting regions were in close proximity using the Bogoliubov-de Gennes equations for superconductivity in a cylindrical nanowire. We succeeded in obtaining the quantum energy levels and wave functions of a superconducting nanowire.

# Nanostructure characterization of multilayered polymers using synchrotron radiation techniques: crystallization phenomena

F. J. Baltá-Calleja, F. Ania, A. Flores

*Instituto de Estructura de la Materia, C.S.I.C.  
Serrano 119, Madrid 28006, Spain*

The presentation offers an overview on recent advances concerning the nanostructure and crystallization behaviour of nanolayered polymer films prepared by layer-multiplying coextrusion, using X-ray scattering techniques. The use of ultra-small angle X-ray scattering (USAXS) reveals the occurrence of scattering maxima corresponding to the nanolayered stacking periodicities. Annealing of crystallisable/amorphous nanolayered films, as in case of PET/PC, induces the crystallization of PET. Consequently the scattering maxima are clearly developed due to an increase in the electron density difference between the alternating polymer layers.

It will be shown that USAXS experiments also reveal an alternating architecture of amorphous polymer nanolayers (for example, PMMA/PS) with a small difference in density. Previous results show that during crystallization from the glassy state the confined crystallization of PET taking place between the amorphous layers of PC is hindered when the thickness of the PET microlayers is confined below the micrometer range. The results also reveal that for pure PET multilayers the appearance of the first WAXS and SAXS peaks occurs at much lower temperatures than when PET is confined between the PC layers. The analysis of data shows that the PET confinement delays the crystallization process. On the other hand, the long period of the crystal lamellar stacks within the PET microlayers increases with decreasing microlayer thickness, while the degree of crystallinity becomes smaller. The results are highlighted on the basis of thinner microlayers giving rise to a smaller density of crystals involving stacks that exhibit larger periodicities.

In case of nanolayered films of two crystalline components (iPP/PA6)(70/30) it will be shown that the crystallization of PA6, being the lower content component, is strongly hindered. It is observed that such a structure continues to influence the crystallization behaviour of both the constituent polymers. On the one hand, the crystallization of PA6 within the multilayered materials is substantially held up, and on the other hand, it is also proposed that the layered morphology of the films induces a preferential orientation of the iPP lamellar structure. The occurrence of a preferential orientation of the  $\alpha$ -form iPP crystals with their c-axes parallel to the layer interfaces (edge-on lamellae) is suggested. Although a slight preferential orientation is observed along the extrusion direction, which probably arises from the first stages of crystallization, the overall iPP orientation seems to be determined by epitaxial growth on the PA6 domain nanostructure.

**References**

- [1] Baltá-Calleja F. J., Ania F., Puente Orench I., Baer E., Hiltner A., Bernal T., Funari S. S. 2005 *Prog. Colloid and Polymer Sci.* **130** 140
- [2] Ania F., Puente Orench I., Baltá-Calleja F. J., Khariwala D., Hiltner A., Baer E., Roth S. V. 2008 *J. Macromol. Chem. & Phys.* **209** 1367
- [3] Puente Orench I., Stribeck N., Ania F., Baer E., Hiltner A., Baltá-Calleja F. J. 2009 *Polymer* **50** 2680
- [4] Flores A., Ania F., Baltá-Calleja F. J. 2009 *Polymer* **50** 729
- [5] Ania F., Baltá-Calleja F. J., Henning S., Hiltner A., Baer E., Khariwala D. 2010 *Polymer* **51** 1805
- [6] Flores A., Arribas C., Fauth F., Khariwala D., Hiltner A., Baer E., Baltá-Calleja F. J., Ania F. 2010 *Polymer* **51** 4530
- [7] Flores A., Ania F., Arribas C., Ochoa A., Scholtyssek A., Baltá-Calleja F. J., Baer E. *Polymer* in press

## Poisson's ratios of $\text{Cu}_2\text{O}$ crystals under temperature changes

V. Belomestnykh, E. Soboleva

*Yurga Institute of Technology of National Research  
Tomsk Polytechnic University  
Leningradskaya 26, 652050 Yurga, Russia*

Copper oxide ( $\text{Cu}_2\text{O}$ , cuprite) demonstrates a number of interesting properties including elastic behaviour under external conditions. For example, both shear constants of the crystal along the specific directions  $\langle 100 \rangle$  and  $\langle 110 \rangle$  –  $c_{44}$  and  $(c_{11} - c_{12})/2$  – have anomalous positive derivatives with respect to the temperature [1,2] and negative with respect to the pressure [3]. Rigidity constants  $c_{11}$ ,  $c_{12}$  and  $c_{44}$  of  $\text{Cu}_2\text{O}$  monocrystals were studied in the low-temperature region ( $T < 300$  K) with the ultrasonic echo-pulse method at the frequencies of 10 MHz and 30 MHz to a precision of 4.3%, 4% and 2.5%, respectively [1]. Four sound velocities along two crystallographic directions under the standard conditions were compared according to the study results in [2]: a good agreement between the velocities of longitudinal waves (for  $v_{L\langle 100 \rangle}$ ) can be noted, the divergences do not exceed 1.6%, for  $v_{L\langle 110 \rangle}$  – 1.5%) and even a better agreement between the velocities of transverse waves can be observed (for  $v_{t\langle 100,001 \rangle}$  the divergences do not exceed 0.2%, for  $v_{t\langle 110,1\bar{1}0 \rangle}$  – 0.9%). Thus, the experimental  $c_{ij}$  of  $\text{Cu}_2\text{O}$  monocrystals can be considered to be a reliable basis for studying the Poisson's ratios of the given compound.

The temperature changes of the Poisson's ratio for the two of them –  $\sigma_{\langle 110,001 \rangle}$  and  $\sigma_{\langle 110,1\bar{1}0 \rangle}$  – are rather significant and oppose each other:  $\sigma_{\langle 100,001 \rangle}$  grows and  $\sigma_{\langle 110,1\bar{1}0 \rangle}$  decreases with a temperature increase. It is possible to suppose that under further temperature increase ( $T \rightarrow T_{\text{melt}}$ ) the Poisson's ratio  $\sigma_{\langle 110,1\bar{1}0 \rangle}$  will have a close to zero value.

However, there is also another possible version. The fact is that the qualitative view of the function  $\sigma_{\langle hkl \rangle} = f(T)$  in  $\text{Cu}_2\text{O}$  somewhat unexpectedly appeared to be almost identical to the “reflection” of the Poisson's ratios of the  $\text{CuCl}$  crystal in the “low” pressure phase ( $p < p_c = 9.75$  GPa, critical pressure of B3 lattice transition into B1 lattice under room temperature) which was obtained earlier [4]. In  $\text{CuCl}$  all Poisson's ratios jump under the transition pressure  $p_c$  and the range of their minimum to maximum values reduces significantly under  $p < p_c$ .

Thus, the results of the study make it impossible to represent the functional relations  $\sigma_{\langle hkl \rangle} = f(T)$  in the temperature interval  $873 - T_{\text{melt}}$  for the  $\text{Cu}_2\text{O}$  crystal, as its polymorphous properties are unknown to the authors. It has been noted above that under linear extrapolation of the Poisson's ratios values under  $T = 873$  K to the melting temperature of copper oxide  $\sigma_{\text{min}\langle 110,1\bar{1}0 \rangle}$  can have its minimum (zero) value. Under the same conditions, the value of another Poisson's ratio for the same crystallographic direction will become maximum and approximately equal  $\sigma_{\text{max}\langle 110,001 \rangle} \approx 0.78$ .

Although the given value exceeds the known theoretical positive limit of the Poisson's ratio for an isotropic solid ( $\sigma + 0.5$ ), it is relevant as there are no limits for possible values of  $\sigma_{\langle hkl \rangle}$ .

**References**

- [1] Hallberg J., Hanson R. C., 1970 *Phys. Status Solidi* **42** 305.
- [2] Berger J., 1978 *Solid State Communic.* **26** 403.
- [3] Manghnani M. H., Brower W. S., Parker H. S., 1974 *Phys. Status Solidi (a)* **25** 69.
- [4] Belomestnykh V., Soboleva E. 2011 *8 Intern. Workshop on Auxetics and Related Systems AUXETICS'11* 97.

## Solvent-based acrylic pressure-sensitive adhesives crosslinked using UV-radiation

Z. Czech, A. Butwin, D. Sowa

*West Pomeranian University of Technology  
Szczecin, Poland*

Acrylics are preferred for the commercially used solvent-based UV-crosslinkable pressure-sensitive adhesive (PSA) systems. They can be used for manufacturing self-adhesive mounting tapes, splicing tapes, labels, protective films, sign and marking films and a wide range of self-adhesive medical products, such as plaster, OP-tapes and diverse biochemical electrodes.

New developed photoreactive acrylic PSAs are characterized by very high tack (initial adhesion), very high adhesion (evaluated as peel adhesion) and excellent cohesion (measured as shear strength).

UV-crosslinkable acrylic PSAs are designed to be crosslinked using UV from a UV lamp or UV radiation emitted by an excimer laser. These products offer high processing speeds, relatively low application viscosity, high resistance to plasticizers and solvents, aggressive tack, and very high heat resistance. Solvent-free UV-crosslinkable acrylic systems such as a second technology platform being offered for solvent replacement are developed based on UV-crosslinkable solvent-based acrylics.

UV-crosslinkable solvent-based acrylic PSAs consist of acrylic copolymers with chemically built-in photoreactive groups. Their molecular weight ranges from 300 000 to 850 000 Daltons and their viscosities are sufficiently low to make the adhesives coatable with standard coating equipment at room temperature. Their performance is comparable or better in comparison with typical solvent-based acrylic PSAs crosslinked using conventional metal chelates or thermal reactive crosslinking agents.

---

# Microstructures of functional polymer nanocomposites fabricated by two-photon photopolymerization

X.-M. Duan

*Laboratory of Organic NanoPhotonics, Technical Institute of Physics and Chemistry  
Chinese Academy of Sciences  
Zhongguancun East Road 29, Beijing 100190, P. R. China*

As an emerging micro/nanofabrication technique, two-photon polymerization (TPP) is promising for fabricating 3D micro/nano-machines due to its capability of 3D micro/nanofabrication and high spatial resolution at nanometric scale [1,2]. The TPP technique has been developed for fabricating micro/nanodevices and micro-electro-mechanical systems (MEMS) [3]. Polymer nanocomposites can play an important role in micro/nanodevices and MEMS [4]. The functionalization of materials is also important in MPP micro/nanofabrication, which can be expected to provide new functions to 3D microstructures. In this paper, we present the latest progress in the fabrication of microstructures, such as polymer/metal nanocomposites.

Micromachines have attracted much interest owing to their extensive applications, such as integrated circuits, wireless communication, microfluidic pumps, and disease diagnosis [5]. Well-designed 3D microstructures could satisfy these requirements. The magnetically driven micromachine has proved promising for remote manipulation and noncontact control. However, the mechanical performance of polymers at micro/nanoscale, such as hardness and strength, is still unknown. Micromachines made of polymers exhibited intrinsically poor mechanical performance, which would limit the potential application in the fields that require mechanical strength, e.g. the elimination of thrombus from blood vessels. We prepared and characterized an Ni-P/polymer composite and demonstrated a method for fabricating 3D micromachines by combining TPP of a polymer and the electroless plating of an Ni-P alloy to achieve high mechanical performance and the capability of remote control. Ni-P electroless plating process was optimized, and the mechanical performance of the Ni-P/polymer composite film, such as hardness and modulus, were improved to 1.74 GPa and 34.93 GPa with the use of an Ni-P alloy layer, which corresponds to a ten-fold and nine-fold improvement, respectively, compared to a polymer film. The fabrication and remote control of magnetic micromachines were carried out based on the understanding of Ni-P/polymer composite materials. We successfully demonstrated that it is possible to remotely manipulate an as-prepared magnetic 3D micromachine by an external magnetic field [6]. This can enable developing remotely manipulated 3D micro/nanomachine with an excellent mechanical performance.

However, in order to develop plasmonic technologies, novel micro/nano-fabrication methods are required to provide complex 3D microstructures, in which the desired ori-

entation and arrangement of metal nanoparticles can be obtained. With this purpose in mind, we investigated plasmonic resonance enhanced two-photon photopolymerization (PETPP) using isolated, chemically synthesized gold nanorods for the fabrication of polymer/metal nanocomposites [7]. The isolated gold nanorods with a plasmonic resonance band around 750 nm covered by a photoresist were irradiated by a femtosecond laser with a wavelength of 780 nm. The PETPP triggered by the plasmonic resonance enhancement of gold nanorods was localized only up to 30 nm from the surface of the gold nanorods, which matched the distance of the plasmonic resonant enhanced field of the gold nanorods. Furthermore, we demonstrate the fabrication of Au nanorod aggregate microstructures by means of a femtosecond near-infrared laser [8]. The laser light was tightly focused onto colloidal Au nanorods dispersed in a photopolymerizable methyl-methacrylate (MMA) compound to induce TPP. TPP of MMA combined the nanorods together, forming solid microstructures of aggregates. The laser light excited a local surface plasmon, resulting in the confinement of TPP in the vicinity of nanorods. Concurrently, the optical accumulation of nanorods created a unique mechanism for the formation of nanorod aggregates into desired microstructures. This technique could be the key to a novel micro/nanofabrication method for plasmonic materials and devices.

## References

- [1] S. Kawata, H. B. Sun, T. Tanaka, K. Takada, *Nature*, **412**, 697, 2001.
- [2] X. Z. Dong, Z. S. Zhao, X. M. Duan, *Appl. Phys. Lett.*, **92**, 091113, 2008.
- [3] X. Z. Dong, Z. S. Zhao, X. M. Duan, *Appl. Phys. Lett.*, **91**, 124103, 2007.
- [4] Z.-B. Sun, X.-Z. Dong, W.-Q. Chen, S. Nakanishi, X.-M. Duan, S. Kawata, *Adv. Mater.*, **20**, 914, 2008.
- [5] R. Kawano, T. Osaki, H. Sasaki, S. Takeuchi, *Small*, **6**, 2100, 2010.
- [6] W.-K. Wang, Z.-B. Sun, M.-L. Zheng, X.-Z. Dong, Z.-S. Zhao, X.-M. Duan, *J. Phys Chem C*, **115**, 11275, 2011.
- [7] K. Masui, S. Shoji, F. Jin, X.-M. Duan, S. Kawata, *Appl. Phys. A: Mater. Sci. Proc.*, **104**, 773, 2012.
- [8] K. Masui, S. Shoji, K. Asaba, T. C. Rodgers, F. Jin, X.-M. Duan, S. Kawata, *Optics Express*, **19**, 22786, 2011.

Influence of graphene on cholesterol lodgment  
localized on protein surface  
– computer simulation study

Z. Gburski, K. Górny, P. Raczyński, M. Pabiszczak

*Institute of Physics, University of Silesia  
Uniwersytecka 4, 40-007 Katowice, Poland*

Cholesterol  $C_{27}H_{45}OH$ , being an essential sterol component of mammalian cell membranes, plays an important role in maintaining physical and mechanical properties of a membrane. Although cholesterol is necessary in mammals' body, its surplus may be unhealthy. For example, it starts the development of foam cells, subsequently leading to the formation of plaque deposition in blood vessels. These plaques are prone to rupture, which can then trigger acute unstable coronary artery syndrome and ischemic stroke. The impact of graphene sheet on the rearrangement of cholesterol molecules, forming a thin layer (lodgment) around the endothelial protein 1LQV, was studied by means of molecular dynamics (MD) simulation. Graphene wall substantially influences the motions of cholesterol and the layer structure. Certain cholesterol molecules migrate from the lodgment and settle down on the graphene surface. As a result, the cholesterol lodgment substantially diminishes due to the graphene intervention.

# Novel synthetic approaches for development of two-dimensional hybrid functional materials

D. Gournis

*Department of Materials Science and Engineering, University of Ioannina  
45110 Ioannina, Greece*

Layered materials represent a diverse and largely untapped source of two-dimensional (2D) nanosystems with high specific surface areas and exceptional physico-chemical properties that are important for applications including without being limited to catalysis, sensing, environmental remediation, biotechnology, and energy storage applications [1]. The nature of the microenvironment between the 2D nanometer size sheets regulates the topology of the intercalated molecules and affects possible supramolecular rearrangements or reactions, such as self-assembling processes that are usually not easily controlled in the solution phase [2]. In this talk, it will be demonstrated how top-down and bottom-up synthetic approaches could be applied to assemble novel hybrid materials based on nanometer size platelets as building blocks. Layered materials (Smectite clays, graphene oxide and graphite nitrate) act as 2D templates for reaction or grafting of a variety of guest species (pure C<sub>60</sub>, fullerene derivatives, cubic silsesquioxanes, adamantane, Prussian Blue analogues) [2–5]. Top-down methods include simple intercalation reactions in bulk where neutral molecules are inserted into either organically modified or not layered matrices and held in the interlayer space by van der Waals interactions or covalent bonding, while positively charged species are introduced into the aluminosilicate clay galleries through ion exchange. Moreover, a new bottom-up approach for the production of two-dimensional functional hybrid materials where layered materials act as the structure directing interface and reaction media will be also presented. This new method, based on combining self-assembly with the Langmuir Schaefer technique, uses layered nanosheets as a template for grafting of guest molecules in a bi-dimensional array, and allows perfect layer-by-layer growth with control at the molecular level. The resulted hybrid layered structures were characterized by a combination of analytical techniques. The experiments gave an insight into the formation process, structural details and properties of the final hybrid structures. Owing to the described fabrication routes it is possible to create entirely novel architectures whose final structure is encoded in the shape and properties of the clusters or molecules that are used.

## References

- [1] Coleman J. N., et al. 2011 *Science* **331** 568
- [2] Gournis D., et al. 2004 *J. Am. Chem. Soc.* **126** 8561; Gournis D., et al. 2006 *J. Am. Chem. Soc.* **128** 6154
- [3] Gengler R. Y. N., et al. 2010 *Small* **6** 35
- [4] Gournis D., et al. 2010 *J. Colloid Interface Sci.* **348**, 393
- [5] Gengler R. Y. N., et al. 2012 *Small*, in press

## EPR study of annealing and rinsing of TiO<sub>2</sub> nanocrystalline materials

N. Gouskos<sup>1,2</sup>, A. Guskos<sup>2</sup>, G. Żołnierkiewicz<sup>2</sup>, J. Typek<sup>2</sup>,  
P. Berczyński<sup>2</sup>, D. Dolat<sup>3</sup>, B. Grzmił<sup>3</sup>, A. Morawski<sup>3</sup>

<sup>1</sup>*Department of Solid State Physics, Faculty of Physics, University of Athens  
Panepistimiopolis, 15 784 Zografou, Athens, Greece*

<sup>2</sup>*Institute of Physics, Faculty of Mechanical Engineering and Mechatronics  
West Pomeranian University of Technology  
Al. Piastów 48, 70-311 Szczecin, Poland*

<sup>3</sup>*Institute of Chemical and Environmental Engineering  
West Pomeranian University of Technology  
Al. Piastów 17, 70-310 Szczecin, Poland*

Samples of TiO<sub>2</sub>, calcined at 500°C (type 1) and 550°C (type 2), were prepared with and without water rinsing. The samples were characterized by XRD and optical spectroscopy. The crystallite sizes were determined to be smaller than 40 nm for both types of samples. The BET specific surface areas for all the samples were about 60 m<sup>2</sup>/g. The very intense EPR spectra of free radicals and titanium ions at low oxidation state were recorded. The temperature dependence of the EPR spectra was calculated for all the samples. The number of oxygen vacancies changed after different thermal and rising annealing processes and, since they were involved in the formation of low oxygenation states of titanium ions, they could be responsible for the appearance of the observed magnetic properties. The photocatalytic activity of samples was studied towards phenol decomposition under UV-Vis and artificial solar light irradiation. It was found that the rinsed materials showed better photocatalytic activity under both types of irradiation. In case of the UV-Vis light irradiation the best was the 500°C/rinsed sample, whereas under artificial solar light the 550°C/rinsed sample was slightly better. All the new materials exhibited better photoactivity than the starting material. The light absorption abilities (UV-Vis/DRS) as well as the surface FTIR/DR studies confirmed significantly enhanced light absorption and the presence of nitrogen groups on the surfaces of the photocatalysts, respectively.

## EPR/FMR studies of cement slurry with different magnetite concentration

N. Gouskos<sup>1,2</sup>, G. Żołnierkiewicz<sup>2</sup>, A. Guskos<sup>2</sup>, J. Typek<sup>2</sup>,  
J. Borucka-Lipska<sup>3</sup>, W. Kiernożycki<sup>3</sup>

<sup>1</sup>*Department of Solid State Physics, Faculty of Physics, University of Athens  
Panepistimiopolis, 15 784 Zografou, Athens, Greece*

<sup>2</sup>*Institute of Physics, West Pomeranian University of Technology  
Al. Piastów 48, 70-311 Szczecin, Poland*

<sup>3</sup>*Department of Concrete Constructions and Technology of Concrete  
Civil Engineering and Architecture Faculty, West Pomeranian University of Technology  
Al. Piastów 50, 70-311 Szczecin, Poland*

Slurries were made on the basis of Portland cement CEM I 42.5 and water with an addition of magnetite in two stages. Firstly, slurries with constant amounts of cement – 450 g and water – 225 g were prepared. At the following stage, magnetite in the amount of 5, 10 and 20 wt.% of the cement was added to the slurry. In the second part of the study the amount of cementite was reduced and replaced by magnetite. All the slurries after mixing were stored at 20°C and humidity of 98%. Under such conditions, the samples matured for 28 days. The aim of this study was to determine the effect of magnetite replacement on the mechanical properties of cement mortar. Tests to determine the compressive strength, bending and binding were carried out. The electron paramagnetic resonance/ferromagnetic resonance (EPR/FMR) investigations of the obtained samples were conducted at room temperature. The first studied sample was a slurry without a magnetite admixture. EPR/FMR lines centered at 3070 G, one with a linewidth of about 1070 G, and another with a linewidth of about 1600 G, were observed. The first line was attributed to magnetic nanoparticles and the second to the isolated Fe<sup>3+</sup> ions in a low symmetry crystal field. The concentration of magnetic nanoparticles was over 30 times smaller than in the samples with additional magnetite. Although the mechanical properties of the slurries with the magnetite addition did not improve, this method could be considered as one of useful applications of magnetite. Cements with magnetite could be also used as magnetic shielding materials.

On the effect of imperfections on the Poisson's ratios  
and other properties of crystalline  
and cellular systems with particular reference  
to their auxetic potential

J. N. Grima<sup>1,2</sup>, R. Gatt<sup>1</sup>, D. Attard<sup>1</sup>, L. Mizzi<sup>1</sup>, J. D. Cutajar<sup>1</sup>,  
A. Casha<sup>2</sup>, R. Cauchi<sup>1</sup>, Ch. Zerafa<sup>1</sup>, R. Caruana-Gauci<sup>1</sup>, B. Ellul<sup>1</sup>,  
M. Camilleri<sup>1</sup>, E. Manicarò<sup>1</sup>, E. Chetcuti<sup>1</sup>

<sup>1</sup>*Department of Chemistry, Faculty of Science, University of Malta  
Msida MSD2080, Malta*

<sup>2</sup>*Metamaterials Unit, Faculty of Science, University of Malta  
Msida MSD2080, Malta*

Auxetics are systems which exhibit a negative Poisson's ratio, i.e. get fatter when stretched and thinner when compressed. This anomalous behaviour is manifested in several honeycombs and cellular structures and may be explained in terms of various geometry/deformation mechanism based models.

Recent developments made by the University of Malta group on imperfect materials and structures are presented and discussed. We show that defects and imperfections in cellular and crystalline systems have a very significant effect on the mechanical properties, in particular the Poisson's ratios.

### **Acknowledgements**

This research work is partly funded by the University of Malta, Malta Council for Science and Technology and by grants awarded to Reuben Cauchi and Christine Zerafa through the Strategic Educational Pathways Scholarship (Malta). These scholarships are part-financed by the European Union – European Social Fund (ESF) under Operational Programme II – Cohesion Policy 2007–2013, “Empowering People for More Jobs and a Better Quality of Life”

# High pressure study of localized states related to $\text{Ln}^{3+}$ and $\text{Ln}^{2+}$ ions in solids

M. Grinberg

*Institute of Experimental Physics, University of Gdansk  
Wita Stwosza 57, 80-952 Gdansk, Poland*

Rare earth ion dopands create luminescence centers in solids. The emission takes place usually due to internal transitions of  $4f^n \rightarrow 4f^n$  and  $4f^{n-1}5d^1 \rightarrow 4f^n$ . The emission can be excited due to the internal absorption ( $4f^n \rightarrow 4f^{n-1}5d^1$  transition), charge transfer transition (CT) or ionization process. In the two latter cases the intermediate states called impurity trapped exciton (ITE) states are created and play an important role in the excitation energy transfer. In this contribution the spectroscopic investigation of luminescence materials doped with several  $\text{Ln}^{3+}$  ( $\text{Ce}^{3+}$ ,  $\text{Pr}^{3+}$ ,  $\text{Eu}^{3+}$ ) and  $\text{Ln}^{2+}$  ( $\text{Eu}^{2+}$ ) is presented. The leading unique experimental technique was the high pressure spectroscopy where high hydrostatic pressure is applied in a diamond anvil cell (DAC). High hydrostatic pressure compresses the materials, leading to an increase in the interaction of the Ln ion with the lattice. This allows changing the energies of the ground states of  $\text{Ln}^{3+}$  and  $\text{Ln}^{2+}$  ions with respect to the band edges of the host as well as the energies of the excited states belonging to the excited electronic manifold  $4f^{n-1}5d^1$  with respect to the ground states of Ln ions. Therefore, high pressure is considered a very effective tool for investigation of influence of ITE states on energy transfer processes in phosphors with  $\text{Ln}^{3+}$  and  $\text{Ln}^{2+}$  ions. The lecture presents a review of recent results on high pressure spectroscopy of  $\text{Ce}^{3+}$ -,  $\text{Pr}^{3+}$ -,  $\text{Eu}^{3+}$ - and  $\text{Eu}^{2+}$ -doped oxide and fluoride phosphors.

---

Three-dimensional Ising model with fluctuating  
exchange integral in asymmetric bimodal  
random field: effective field theory  
– differential operator technique

I. Hadjiagapiou

*Department of Solid State Physics, Faculty of Physics, University of Athens  
Panepistimiopolis, 15 784 Zografou, Athens, Greece*

The spin-1/2 Ising model on a cubic lattice, with fluctuating pair interactions between nearest neighbors and in the presence of random magnetic fields, is investigated within the framework of the effective field theory, based on the use of the differential operator relation  $e^{wD}f(x) = f(x+w)$ , where  $D$  is the differential operator. The random field is drawn from the asymmetric and anisotropic bimodal probability distribution  $P(h_i) = p\delta(h_i - h_1) + q\delta(h_i + ch_1)$ , where the site probabilities  $p$ ,  $q$  take on values from the interval  $[0, 1]$  such that  $p + q = 1$ ;  $h_i$  is the random field variable with a strength  $h_1$  and  $c$  is the competition parameter, i.e. the ratio of the respective strengths in the two principal directions,  $+z$  and  $-z$ , which is positive and results in competing random fields. Moreover, the fluctuating pair interactions are drawn from the symmetric, but anisotropic, bimodal probability distribution  $P(J_{ij}) = (1/2) \{ \delta(J_{ij} - (J + \Delta)) + \delta(J_{ij} - (J - \Delta)) \}$ , where  $J$  and  $\Delta$  represent the average value and standard deviation of  $J_{ij}$ , respectively. We estimated transition temperatures, phase diagrams (for various values of system parameters  $c$ ,  $p$ ,  $h_1$ ,  $\Delta$ ), susceptibility, and the equilibrium equation for magnetization, which is solved in order to determine the magnetization profile with respect to  $T$ ,  $h_1$  and  $\Delta$ .

# A 2-constituent system displaying negative effective Poisson's ratio and negative effective stiffness

T. A. M. Hewage, K. L. Alderson, A. Alderson

*Institute for Materials Research and Innovation, University of Bolton  
Deane Road, Bolton BL3 5AB, UK*

Negative, or anomalous, materials are of interest for their counterintuitive behaviour and because they can offer a route to developing composite materials showing extreme values of properties not achievable via conventional materials. Examples of materials displaying negative properties include negative Poisson's ratio (NPR), negative thermal expansion (NTE) and negative stiffness (NS) materials.

Negative Poisson's ratio (Auxetic) materials expand when stretched and contract when compressed. A number of Auxetic materials have been developed, including foams, fibres and films. Properties enhanced by the presence of a negative Poisson's ratio include shear modulus, fracture toughness and impact resistance.

Negative stiffness is another interesting negative property, corresponding to a reversal of the direction of the applied force to the direction of the displacement and can occur in objects such as buckled beams and in ferroelastic materials. It has been reported that negative stiffness can be used in systems to enhance vibration damping response.

This paper will report on a 2-constituent composite system which displays both negative effective Poisson's ratio and negative effective stiffness. Generalized analytical expressions have been derived for the Poisson's ratio and Young's modulus of the NS-NPR system. The dependencies of the Young's Modulus and Poisson's ratio values with the global strain will be presented in 3D plots for different combinations of the design variables.

## **Acknowledgements**

This material is based upon work supported by, or in part by, the U.S. Army Research Laboratory and the U.S. Army Research Office under grant number W911NF-11-1-0032.

# Possible auxeticity in some natural solid/liquid systems

A. R. Imre

*HAS Centre for Energy Research  
POB49, Budapest, H-1525 Hungary*

Auxeticity can be caused by purely structural (geometrical) reasons, nevertheless sometimes other factors can contribute as well. It has been known for some time that in some liquid/solid systems where the liquid is confined into cells with solid walls, auxeticity can occur when the liquid part is under negative pressure [1]. The negative pressure states being metastable for liquids, it is not possible to build these structures easily [2]. In this talk, we would like to propose some natural capillary systems (biological and geological), where auxeticity could occur due to the relative position of capillaries and the existence of negative capillary pressure. Some consequences of auxeticity in these systems will be also discussed.

## References

1. K. W. Wojciechowski 1995 Mol. Phys. Rep. 10, 129
2. A. R. Imre 2006, Phys. Stat. Sol. b, 244, 893

## Structural and luminescent properties of microwave hydrothermal synthesized ZrO<sub>2</sub> nanopowders

J. Kaszewski<sup>1</sup>, S. Yatsunenکو<sup>2</sup>, M. Godlewski<sup>2</sup>, I. Pełech<sup>1</sup>,  
P. Łukaszcuk<sup>1</sup>, E. Mijowska<sup>1</sup>, G. Żołnierkiewicz<sup>3</sup>, N. Gouskos<sup>3,4</sup>,  
E. Kusiak<sup>1</sup>, J. Orlikowski<sup>1</sup>, W. Morawski<sup>1</sup>, U. Narkiewicz<sup>1</sup>

<sup>1</sup>*Institute of Chemical and Environment Engineering  
West Pomeranian University of Technology  
Pulaskiego 10, 70-322 Szczecin*

<sup>2</sup>*Institute of Physics of the Polish Academy of Sciences  
Al. Lotników 32/46, 02-668 Warsaw, Poland*

<sup>3</sup>*Institute of Physics, Faculty of Mechanical Engineering and Mechatronics  
West Pomeranian University of Technology  
Pulaskiego 17, 70-322 Szczecin*

<sup>4</sup>*Department of Solid State Physics, Faculty of Physics, University of Athens  
Panepistimiopolis, 15 784 Zografou, Athens, Greece*

The hydrothermal method is commonly applied for the synthesis of oxide nanopowders with new advanced properties. The method may be modified by the application of microwave heating. Microwave heating allows to obtain high quality powders with the application potential in oxygen sensors, fuel cells and catalysts [1]. Other advantages of hydrothermal materials processing are: high purity of the products, high reaction rates, low grain size dispersion, control of the grain shape, synthesis without pollution, energy and space saving, low temperature of process [2]. A short time of process and high purity environment resulting from using microwaves instead of heating elements of any kind are additional advantages of the method [3].

Zirconium dioxide is an excellent material for optical applications. Its hardness, high chemical stability, optical transparency and high refractive index make it perfect for application in optoelectronics, biotechnology and medical sciences. Pure and yttria stabilised zirconia are excellent hosts for rare earth ions [4].

In the present work pure zirconia nanopowders have been synthesized via microwave hydrothermal process at the pressure of 5.5 MPa. The starting zirconium compound (ZrO(NO<sub>3</sub>)<sub>2</sub>·xH<sub>2</sub>O, Aldrich, x≈6) was dissolved in distilled water. Then, the pH was adjusted to the value of 10 by a rapid addition of ammonia water solution. The residue was then washed and placed in the teflon vessel of the microwave hydrothermal reactor. After 20 minutes the reaction was stopped and the powders were dried. Then, nanopowders were characterised by means of XRD, TEM, Raman spectroscopy, UV/Vis spectroscopy and EPR. It was found that fine nanocrystalline zirconia powders with a narrow grain size distribution were obtained. The powder was calcined at the temperatures of 400, 800 and 1200°C. The volume fraction of monoclinic zirconium dioxide phase has increased exponentially in the function of the

heating temperature. The sample calcined at 1200°C was found to be pure monoclinic zirconia with the average grain size of 60 nm. The obtained material was highly agglomerated. TEM observations were generally in a good agreement with the grain size calculations from XRD patterns. The band gap in the obtained material depended on the heating temperature from 3.02 to 4.72 eV. The intensity of luminescence has increased significantly after calcination and depended on the heating temperature. EPR measurements have been conducted at room temperature. Some of them have shown paramagnetic centers (arising from defects) which could play an important role on the material's physical properties.

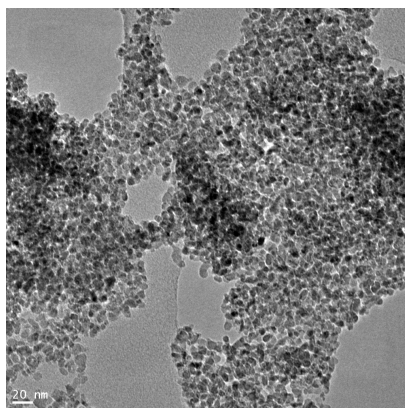


Figure 1: HRTEM image of the  $\text{ZrO}_2$  sample annealed at 400°C

## References

- [1] Kumari L., Du G. H., Li W. Z., *Synthesis, microstructure and optical characterization of zirconium oxide nanostructures*, Selva Vennila R., Saxena S. K., Wang D. Z., *Ceramics International*, **35**, 2401–2408, 2009
- [2] Somiya S., Akiba T., *Hydrothermal Zirconia Powders: A Bibliography*, *Journal of the European Ceramic Society* **19**, 81–87, 1999
- [3] Byrappa K., Adschiri T., *Hydrothermal technology for nanotechnology*, *Progress in Crystal Growth and Characterization of Materials* **53**, 117–166, 2007
- [4] Kumari L., Li W. Z., *Controlled hydrothermal synthesis of zirconium oxide nanostructures and their optical properties*, *Crystal Growth and Design* **9**, 3874–3880, 2009

## Localization of carriers and spins in nanocarbons

W. Kempański<sup>1</sup>, M. Kempański<sup>2</sup>, D. Markowski<sup>1</sup>, Sz. Łoś<sup>1</sup>

<sup>1</sup>*Institute of Molecular Physics, PAS  
Smoluchowskiego 17, 60-179 Poznań*

<sup>2</sup>*Faculty of Physics, A. Mickiewicz University  
Umultowska 85, 61-614 Poznań*

The localization phenomenon is studied for spins and carriers in different modern nanocarbon materials: C<sub>60</sub> fullerenes, carbon nanotubes or graphene based materials such as activated carbon fibers in which an arrangement of the quantum dot matrix could be observed.

Two basic experimental methods are used to define the localization of spins or carriers and their population control in nanocarbon materials: electron paramagnetic resonance and DC electrical conductivity. Experimental results will be discussed in a frame of possible applications in molecular electronics or spintronics.

### **Acknowledgements**

This research was partially supported by Polish grant MNiSW DPN/N174/COST/2010 and COST MP0901 "NanoTP".

---

# Multiphase reactive blends based on thermoplastic polyester

K. Kwiatkowski, M. Kwiatkowska

*Institute of Materials Science and Engineering  
West Pomeranian University of Technology Szczecin  
Al. Piastów 17, 70-310 Szczecin, Poland*

Preparation of multiphase polymer blends as a way to obtain materials with improved or quite new features makes an alternative for the cost and time consuming research on synthesis of new homopolymers with defined functionality. It does not require sophisticated equipment and it is not harmful for the environment, while the obtained materials may find many applications in different fields, where easy processing and specified physical properties are desired. What is also important, waste polymer materials can be also used as blend components.

Thermoplastic polyesters due to their various physical properties are considered as engineering materials, however, they are also components of thermoplastic elastomers (TPE) – a special kind of polymer materials combining rubber-like elasticity with processability typical for thermoplastics. When condensed, TPE exhibit a nanodomain structure consisting of two phases: hard and soft. The continuous soft phase is made by flexible polymer chains with relatively low glass transition temperature ( $T_g$ ) (flexible segment), whilst the hard phase is created by rigid segments with relatively high  $T_g$ , able to crystallize or make hydrogen/ionic bonds between macromolecules. In consequence, when the material is loaded by an external force it is only the soft phase that is deformed, and crystallites of rigid segments – playing the role of physical network nodes – make it thermoreversible and easily processable. An example of such TPE materials are commercially available poly(ether-ester) copolymers based on PBT and polyoxytetramethylene (PTMO), obtained in two-step synthesis: transesterification and polycondensation. A similar process was employed to obtain copolymers based on PET, however, due to the lower ability to crystallization, these materials have been not commercialized yet. An alternative approach to the conventional polycondensation process in polyester elastomers seems to be reactive blending or reactive compatibilization. It consists in creating specified conditions to enable chemical reactions *in situ* between two polymeric components in the molten state and the resulting blend has a stable, multiphase and thermoreversible structure with all the features of thermoplastic elastomers.

The studies on the conditions of preparation and characterization of PET-PTMO reactive blends, proving that the obtained material has a structure of copolymer with phase separation and physical properties very close to the commercial TPE, are presented here. The special interest was the application of waste PET materials as copolymer rigid segments.

## **Acknowledgements**

The research was financed by the Polish Ministry of Science and Higher Education from the resources for the years of 2009–2011 as a research project.

# Towards quantum limits in scaling of electronic devices

W. Nawrocki

*Faculty of Electronics and Telecommunications  
Poznan University of Technology  
60-965 Poznan, Poland*

## Introduction

In this paper some physical limits for the scaling of devices and conducting paths inside semiconductor integrated circuits (ICs) are discussed. Semiconductor technologies, mostly CMOS and TTL, have been used to fabricate integrated circuits on an industrial scale for the last 40 years or so. The CMOS technology will probably be used at least for another 10–15 years. A forecast of the development of the semiconductor industry (ITRS 2009) predicts that the sizes of electronic devices in ICs will become smaller than 10 nm in the next 10 years [1]. The physical gate length of a MOSFET may even amount to 7 nm in the year 2024. At least 5 physical effects should be taken into account when discussing the limits of miniaturization of ICs:

- quantization of both electrical and thermal conductance in narrow and thin channels in transistors and in conducting paths;
- spread of doping atoms in a semiconductor material; each dopant atom would induce a relatively high potential bump;
- propagation time of an electromagnetic wave along and across a chip (IC);
- electrostatics; loss of electrostatic control over the drain current vs. the gate voltage;
- electron tunneling between a source and a drain inside a MOSFET through an insulation (oxide).

## Quantization of electrical conductance

Electrical and thermal properties of electronic devices or paths with nanometer sizes are no longer described by the classical theory of conductance, but rather by quantum theories. The theoretical quantum unit of electrical conductance  $G_0 = 2e^2/h$  was predicted by Landauer in his theory of electrical conductance [2]. For a 1-D system, with a thickness  $H \leq \lambda_F$ ,  $N$  depends on the width of the wire,  $N = \text{int}(2W/\lambda_F)$ ,  $\lambda_F$  – Fermi length. For a 2-D system, with  $H, W \geq \lambda_F$ ,  $N = \text{int}(W \times H/\lambda_F^2)$ , where  $\text{int}(A)$  is the integer of  $A$ . However, defects, impurities and irregularities of the shape of the conductor can induce scattering, in which case the conductivity is given by the Landauer equation (1).

$$G = \frac{2e^2}{h} \sum_{i,j=1}^N t_{ij}, \quad (1)$$

where  $N$  is the number of transmission channels,  $t_{ij}$  denotes the probability of the transition from the  $j^{\text{th}}$  to the  $i^{\text{th}}$  state.

The quantization of electric conductance depends neither on the kind of element nor on temperature. For conductors and semiconductors the conductance quantization, in units of  $G_0 = 2e^2/h = (12.9 \text{ k}\Omega)^{-1}$ , was measured in many experiments.

We investigated nanowires made of pure metals and metallic alloys. In our experiments, the quantization of conductance was evident. Fig. 1 (left panel) presents plots of electrical conductance versus time for gold nanowires and for a junction: cobalt tip – germanium plate. The intensity of the dynamic formation of nanowires is shown in the form of histograms (right panel).

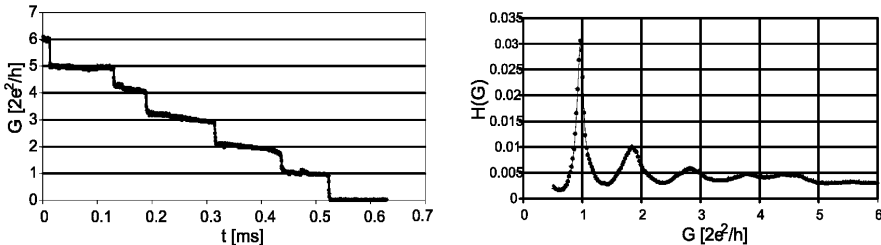


Figure 1: Conductance quantization in gold nanowires and quantization intensity (histograms)

Let's consider a silicon path with a length  $L = 20 \text{ nm}$  ( $L < \Lambda_{\text{Si}}$ ), width  $W = 3 \text{ nm}$ , thickness  $H = 3 \text{ nm}$  and  $\lambda_F = 1 \text{ nm}$ . Such a path is a nanowire with the conductance  $G_P = 7.75 \cdot 10^{-5} \cdot 9 = 7 \cdot 10^{-4} \text{ [A/V]}$ . The resistance of the path is  $R_P = 1/G_P = 1.43 \text{ k}\Omega$ , which is surprisingly high. The electrical capacity of the path is  $2 \text{ pF/cm}$  [1], thus for  $L = 20 \text{ nm}$ ,  $C_P = 4 \cdot 10^{-18} \text{ F}$ . The path inside an IC forms a low-pass RC filter with an upper frequency of  $f_u = 1/(2\pi R_P C_P) \approx 3 \cdot 10^{13} \text{ Hz}$ , and thus the path filters out signals.

### Quantization of thermal conductance

Limits the for speed-up of digital circuits, especially microprocessors, are determined by thermal problems. There are several analogies between the electrical ( $G_E$ ) and thermal ( $G_T$ ) conductance of a nanostructure. However, the analysis of thermal conductance is more complex than of the electrical conductance because of the contribution of both phonons or electrons to heat exchange. The quantization of thermal conductance in one-dimensional systems was predicted theoretically by Greiner [3] for the ballistic transport of electrons and phonons. The quantized thermal conductance  $G_T$  and its quantum (unit)  $G_{T0}$  was confirmed experimentally by Schwab [4]. The quantum of thermal conductance

$$G_{T0} \text{ [W/K]} = (\pi^2 k_B^2 / 3h) T = 9.5 \cdot 10^{-13} T \quad (2)$$

depends on temperature (2). At  $T = 300 \text{ K}$ ,  $G_{T0} = 2.8 \cdot 10^{-10} \text{ [W/K]}$ .

A single nanowire should be considered together with its terminals. Electron transport in a nanowire is ballistic, which means that the transport takes place without the scattering of electrons and without energy dissipation. Energy dissipation occurs in terminals. Because of the energy dissipation, local temperature  $T_{\text{term}}$  in terminals is higher than the temperature  $T_{\text{wire}}$  of the nanowires themselves.

### Spread of doping atoms in a material

Classical theories of electrical and thermal conductance assume a huge number of atoms and free electrons. Let's assume a silicon cube with a length of  $a$  and a common doping level of  $10^{16} \text{ cm}^{-3}$ . In an  $n$ -doped silicon cube with a size of  $(100 \text{ nm})^3$  there are  $5 \cdot 10^7$  atoms and 10 free electrons at 300 K, but in an Si cube with the size of  $(10 \text{ nm})^3$  there are  $5 \cdot 10^4$  atoms and only a 1% chance of finding one free electron. This means that common doping in a semiconductor material is insufficient for electronic nanodevices. In order to retain the conductive properties of a semiconductor material, more intensive doping, e.g.  $10^{20} \text{ cm}^{-3}$  must be applied. However, such intensive doping dramatically decreases the resistivity of the material from  $2 \cdot 10^{-3} \Omega\text{m}$  to  $10^{-5} \Omega\text{m}$  (for  $n$ -type Si, at 300 K). A small number of free electrons is expected to be scattered evenly in the entire volume of the material.

### Other physical limits

The channel length  $L_E$  of Si MOSFET, limited by the degradation of electrostatic control in a transistor, was analyzed by Likharev [5]. The shortest channel length  $L_E$  depends on the thickness of the channel  $H_{\text{ch}}$ , the thickness of the insulation layer  $H_i$ , dielectric constants of the channel  $\varepsilon$  and the insulation  $\varepsilon_i$  – formula (3), see Fig. 2 [5]. If we take assume the ratio  $\varepsilon_i/\varepsilon \approx 0.3$  (for silicon oxide and silicon),  $H_{\text{ch}} = 2 \text{ nm}$ ,  $H_i = 1.5 \text{ nm}$  – the estimated minimum length of the channel is  $L_E \approx 3 \text{ nm}$ . The channel length  $L_E$  can be shorter, if a better insulator than silicon oxide ( $\text{SiO}_2$ ) is applied, e.g. silicon nitride, hafnium oxide or zirconium silicate.

$$L_E = \left( \frac{\varepsilon H_{\text{ch}} H_i}{2\varepsilon_i} \right)^{1/2} \quad (3)$$

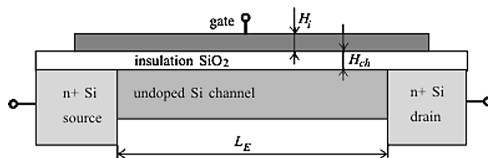


Figure 2: MOSFET transistor – simple model

Another limit of the miniaturization of electronic devices comes from source to drain tunneling through the potential barrier along the channel. The tunneling effect depends on the channel length  $L$  and the supply voltage. Because of tunneling, the minimum channel length for a silicon device is around 2 nm [5].

### Conclusions

Several physical effects must be taken into account for the miniaturization of electronic circuits. The most important ones are: the quantization of electrical and thermal conductance in nanostructures, degradation of electrostatic control in the channel of MOSFET and tunneling along the channel of MOSFET. Conductance quantization was observed in a simple experimental setup, giving the opportunity to investigate subtle quantum effects in electrical conductivity. The energy dissipation in nanowires takes place in their terminals. Other physical effects that are important for

scaling were analyzed theoretically and simulated. According to the state of the art, the minimum length of gate in MOSFET in silicon integrated circuits is around 3 nm.

## References

- [1] International Technology Roadmap for Semiconductors, Edition 2011, <http://www.itrs.net/reports>.
- [2] R. Landauer, *J. Phys.: Cond. Matter* 1, 8099 (1989).
- [3] A. Greiner, L. Reggiani, T. Kuhn and L. Varani, *PRL* 78, 1114 (1997).
- [4] K. Schwab, E. A. Henriksen, J. M. Worlock and M. L. Roukes, *Nature* 404, 974 (2000).
- [5] K. Likharev, Likharev K 2003 *Advanced Semiconductor and Organic Nano-techniques*, ed. Markoç H., Amsterdam: Elsevier, chapter 4 (2003).

---

## Structure, magnetic properties and FMR spectroscopy of Ni-Al nanoferrites

B. V. Padlyak<sup>1,3</sup>, A. V. Kopayev<sup>2</sup>, Yu. N. Tafiychuk<sup>2</sup>,  
D. L. Zadnieprianniy<sup>2</sup>, A. Drzewiecki<sup>1</sup>

<sup>1</sup>*Division of Spectroscopy of Functional Materials  
Institute of Physics, University of Zielona Góra  
Szafrana 4a, 65-516 Zielona Góra, Poland*

<sup>2</sup>*Vasyl Stefanyk PreCarpathian National University, Physical-Technical Faculty  
Shevchenky 57, 76-000 Ivano-Frankivsk, Ukraine*

<sup>3</sup>*Institute of Physical Optics, Sector of Spectroscopy  
Dragomanova 23, 79-005 Lviv, Ukraine*

The Ni-Al polycrystalline ferrites reveal very interesting physical properties and are promising materials for microwave and magneto-electronic devices. The crystal structure, magnetic structure and properties of the Ni-Al ferrites essentially depend on their chemical composition and cationic distribution in the octahedral and tetrahedral sites, caused by the technological conditions of their synthesis. The transition from massive (bulk) Ni-Al ferrites to nanosized materials with particle dimensions comparable and close to interatomic distances essentially changes their magnetic structure and properties. In the presented work, the crystal structure, the magnetic structure and the properties of the Ni-Al nanoferrites were investigated by different methods.

The powdered nanoferrites of the  $\text{NiAl}_x\text{Fe}_{2-x}\text{O}_4$  ( $x = 0, 0.5, 0.68, 0.74$ ) compositions were obtained by a nanotechnology process using the sol-gel method accompanied by auto-combustion. The X-ray analysis showed that all the obtained Ni-Al nanoferrites practically belonged to the single phase compounds with a spinel structure. The technological conditions of the Ni-Al nanoferrites synthesis led to a change of the nanoparticle size. The size of the particles in the obtained Ni-Al nanoferrites evaluated using the X-ray data and Scherer's formula lay in the 25 to 50 nm.

The XANES (X-ray Absorption Near Edge Structure) spectroscopy showed that iron was incorporated into the crystal lattice of the Ni-Al nanoferrites in the trivalent state ( $\text{Fe}^{3+}$ ). The magnetic structure of the Ni-Al nanoferrites was investigated using Mössbauer spectroscopy. In particular, it was shown that the area and parameters of the  $^{57}\text{Fe}^{3+}$  paramagnetic doublet which was observed in the background of the  $^{57}\text{Fe}^{3+}$  sextet belonging to magnetic ordered phase, essentially depended on the technological conditions of the nanoferrites preparation.

The magnetic properties of the obtained Ni-Al ferrite nanopowders were investigated using the magnetic susceptibility measurements at low frequencies and ferromagnetic resonance (FMR) spectroscopy in the microwave X-band ( $\nu \cong 9.4$  GHz) range. The magnetic susceptibility of the Ni-Al ferrite nanopowders showed a linear dependence on the nanoparticle size that correlated to the calculated data. The

lineshape and maxima position of the experimental FMR signals and their parameters (g-factor, gyromagnetic ratio, and peak-to-peak derivative linewidth) for all the obtained Ni-Al ferrite nanopowders were determined and analyzed. The possibilities of determination by FMR spectroscopy in different microwave bands of the saturation magnetization, magnetocrystalline anisotropy, and demagnetization factors for nanoferrites and other magnetic nanoparticles were considered and discussed.

## **Acknowledgements**

This work was supported by the Vasyl Stefanyk PreCarpathian National University (Ukraine) and the University of Zielona Góra (Poland).

# Real time quantum tunneling

G. J. Papadopoulos

*Department of Physics, Solid State Physics Section, University of Athens  
Panepistimiopolis, Athens 157 84 Zografos, Athens, Greece*

A real time scheme for the tunnelling effect past a barrier, within the semi-classical approximation, as a first step, is presented. The semi-classical propagator across a truncated hyperbolic barrier is obtained analytically in terms of the energy required for a particle to flee from a given position on one side of the barrier to a given position on the other side in a specified time. Given the particle's initial state in the form of a wave packet the propagator is used to obtain the wave function on the barrier's other side. The wave function, then, supplies both the probability and current densities as they evolve in time.

# Pillaring of GO by stabilized cationic benzidine free radicals

D. Petridis<sup>1</sup>, E. C. Vermisoglou<sup>1</sup>, N. Todorova<sup>1</sup>, T. Giannakopoulou<sup>1</sup>,  
N. Gouskos<sup>2</sup>, C. Trapalis<sup>1</sup>

<sup>1</sup>*Institute of Advanced Materials, Physicochemical Processes, Nanotechnology and Microelectronics, National Centre for Scientific Research "Demokritos" 153 10, Aghia Paraskevi, Attikis, Greece*

<sup>2</sup>*Department of Solid State Physics, Faculty of Physics, University of Athens Panepistimiopolis, 15 784 Zografou, Athens, Greece*

Benzidine, the aromatic diamine, undergoes oxidative intercalation into layers of graphite oxide, GO, forming a pillared structure in which stabilized benzidine free radicals pin the GO layers. In the course of intercalation the benzidine molecule is grafted to the GO layers by a nucleophilic reaction with the epoxy groups of the host layers, while the guest benzidine donates an electron to the graphite layer and is converted to a cationic free radical stabilized in the interlayer region. The mode of intercalation between GO and benzidine is investigated by XRD (Fig. 1), TEM, FTIR while the generation of the free radical by ESR.

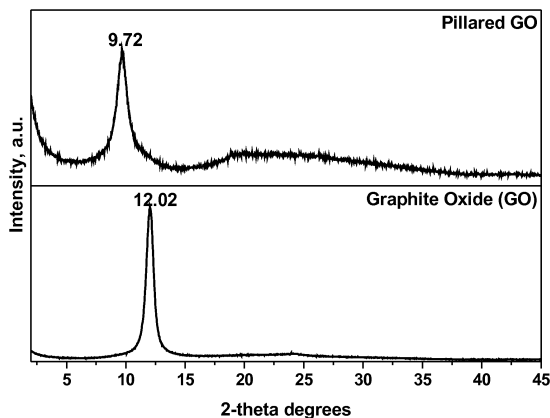


Figure 1: XRD pattern of graphite oxide (GO) and pillared GO with benzidin.

# Cooperative dynamics in frame of a dynamic lattice liquid (DLL) model as a tool to simple and complex liquids simulations

P. Polanowski

*Department of Molecular Physics, Lodz Technical University  
Zeromskiego 116, 90-924 Lodz, Poland*

A computer simulation has become one of the major tools in material science which provides an insight into molecular structures and dynamic behavior under various conditions. There are many algorithms for a simulation of simple and complex liquids (polymer solutions, gels, blends, etc...) on a lattice, but only few of them can work with the density factor  $\rho = 1$  (such a statement indicates that each lattice site is occupied by one monomer unit) and which can properly reflect the dynamics over a broad time range. The dynamic lattice liquid (DLL) model can work with the density factor  $\rho = 1$  and become a basis for the first parallel algorithm which takes into account coincidences of elementary molecular movements resulting in a local cooperative transformation. We present investigation of dynamic and static properties of a simple liquid and polymer solution for various situations obtained by using a simulation based on the DLL model [1–5].

## Acknowledgements

This work was supported by NCN Poland under Grant No. 2011/01/B/ST5/06319.

## References

- [1] Polanowski P., Pakuła T. 2004 *J. Chem. Phys.* **120** 6306.
- [2] Polanowski P., Koza Z. 2006 *Phys. Rev.* **74** 36103.
- [3] Polanowski P. 2007 *J. Non. Cryst. Sol.* **353** 4575.
- [4] Gao H., Polanowski P., Matyjaszewski K. 2009 *Macromolecules* **42** 5929.
- [5] Polanowski P., Jeszka J. K., Matyjaszewski K. 2010 *Polymer* **51** 6084.

# Amorphous and nanocrystalline ferromagnetic microwires enabled multifunctional composites

F. X. Qin<sup>1</sup>, H. X. Peng<sup>1,2</sup>

<sup>1</sup>*Advanced Composite Center for Innovation and Science (ACCIS)  
Department of Aerospace Engineering, University of Bristol  
University Walk, Bristol, BS8 1TR, UK*

<sup>2</sup>*Bristol Centre for NanoScience and Quantum Information (NSQI)  
University of Bristol  
Tyndall Avenue, Bristol, BS8 1DF, UK*

The amorphous ferromagnetic microwires have aroused much interest for a range of engineering applications such as microwave absorption, EMI shielding [1,2]. From fundamental point of view, the ferromagnetic microwire has large permeability and appreciable conductivity and fine size, enabling the contribution of both magnetic loss and electrical loss with a relatively lightweight structure, hence meet the essential requirement of effective absorption at gigahertz frequency spanning S-band, X-band and Ku band. In comparison with other absorbents such as the intensively researched magnetic ferrites powders, ferromagnetic microwires are advantageous in their unique shape anisotropy that aids wave attenuation and superior tailorability of electromagnetic properties through wire geometry and concentration. Herein, to the best of our knowledge, we conduct the first study of the microwave absorption properties of the composites containing Fe-based glass-covered ferromagnetic amorphous microwires embedded in an aerospace-grade E-glass/epoxy prepreg matrix. These new composites exhibit excellent absorption of up to 22.8 dB for a very low filler loading of up to 0.1 wt%.

Experimentally, we embedded glass-covered Co-based and/or Fe-based microwires of different geometry into the E-glass reinforced polymer matrix (#950) of an in-plane size of  $300 \times 200$  mm and unidirectional glass fibre, with two kinds of wire geometries, namely, random short-wire composite and parallel continuous-wire composite. The unidirectional GFRP laminates exhibits an orientation preference to the absorption due to the polarization effect of glass fibres and a positive dependence of absorption on the number of laminate by reaching 10 dB for 10-layer laminates. This is very well explained by an equivalent circuit model consisting of parallel connected resistive and capacitive elements. With wires addition, there appears a remarkable dependence of microwave absorption performance on the local properties of wires such as wire geometry, the mesostructure such as inter-wire spacing, wire orientation, wire pattern (short random or long continuous) and wire concentration as well as the embedded depth of the wires layer. All these observed effects are elucidated within the framework of microwave absorption theory as well as some latest models that were experimentally testified in our previous work [3,4]. Based on the analyses of these results, we propose an optimized design of the microwire/GFRP composites to achieve simultaneous

highest possible absorption and impact performance for multifunctional applications in aeronautical structures and wind turbines.

**References**

1. M. H. Phan, H. X. Peng, *Prog Mater Sci.* **53**, 323–420 (2008).
2. F. X. Qin, H. X. Peng, *Prog Mater Sci* 10.1016/j.pmatsci.2012.06.001 (2012).
3. F. X. Qin, C. Brosseau, H. X. Peng, *Applied Physics Letters*, **99**, 252902, 1–4 (2011).
4. F. X. Qin, C. Brosseau, H. X. Peng, H. Wang, J. Sun, *Appl Phys Lett* **100**, 192903 (2012).

# Nanoscale origins of thermally-driven strain recovery in some shape-memory liquid crystalline networks

W. Ren, P. J. McMullan, W. Kline, A. C. Griffin

*School of Materials Science and Engineering  
Georgia Institute of Technology  
Atlanta GA 30332-0295 USA*

By a self-assembly process, a polydomain liquid crystalline (SmC) phase has been produced in a series of main-chain liquid crystalline network films. Uniaxial stretching of these films at room temperature produces a monodomain structure that can, upon removal of load, retain a significant level of the imposed strain. Although these films show ordinary elastic response at temperatures in the mesophase near the isotropization (clearing) temperature, at room temperature – far below the clearing temperature – the mechanical response is anelastic. If stretched above a threshold strain, the films do not fully recover their original dimensions after unloading.

We will present results showing strain retention as a function of time after removal of load. We will concentrate the presentation on the temperature profile of the strain recovery process. It appears that thermal strain recovery in these materials is closely correlated with the change in global order parameter of the monodomain structure. Of particular interest is the origin of anelasticity in these films and the mechanistic length scale responsible for strain retention and strain release in these networks.

Upon heating the monodomain network from room temperature, recovery of the original film dimensions occurs. The strain recovery (length) curves show a pronounced curvature as the temperature approaches the smectic-isotropic temperature. It is proposed that nanosegregation of netpoints in the smectic structure is responsible for the anelasticity and that the temperature dependence of the shape recovery is consistent with a balance between enthalpic and entropic forces as the temperature increases. The issue of whether it is possible to predict detailed mechanical response in liquid crystalline networks from knowledge of their complex macromolecular chemical architecture will be addressed in terms of hierarchical structures intrinsic to such networks.

# Similarity of fluctuations of critical systems in natural time

N. V. Sarlis

*Solid State Section, Physics Department, University of Athens  
Panepistimiopolis, 15 784 Zografou, Athens, Greece*

Natural time analysis, introduced almost a decade ago [1,2], provides a general framework for the study of complex systems [3]. In a time series of individual events, e.g., avalanches, the natural time associated with the  $k$ -th event is given by  $\chi_k = k/N$ , where  $N$  is the total number of avalanches. The pair  $(\chi_k, Q_k)$ , where  $Q_k$  is the energy associated with the  $k$ -th event, is studied by means of the distribution  $p_k = Q_k/\sum Q_n$  which reflects normalized energy for the  $k$ -th event. It turns out that the variance of natural time  $\kappa_1 \equiv \langle \chi^2 \rangle - \langle \chi \rangle^2$ , where  $\langle \dots \rangle$  denote averages with respect to the distribution  $p_k$ , is of crucial importance for identification of the approach of a complex system to criticality [4]. The quantity  $\kappa_1$  may serve as an order parameter for seismicity and its fluctuations relative to the standard deviation of its distribution were studied [5]. We find that the scaled distributions for various seismic areas – as well as that of the world-wide seismicity [6] – fall on the same curve, which, interestingly enough, exhibits, over four orders of magnitude, an exponential tail similar to that observed in several equilibrium critical phenomena (e.g. the two-dimensional Ising model), as well as in nonequilibrium systems (e.g. the three-dimensional turbulent flow). By analyzing the time series of a ricepile evolving to self-organized criticality or the magnetic flux penetration in thin films of  $\text{YBa}_2\text{Cu}_3\text{O}_{7-x}$ , we show that the scaled distributions for the variance  $\kappa_1$  also exhibit a similar exponential tail [7]. Moreover, entropy  $S$  can be defined in natural time [8,9], which exhibits positivity, concavity and experimental robustness [10]. In general, the value of  $S$  changes [10] upon time reversal to a value denoted by  $S_-$ , thus providing information whether the system evolves into a new state. For the evolving ricepile  $S_-$  is systematically larger than the entropy  $S$  in natural time, while in  $\text{YBa}_2\text{Cu}_3\text{O}_{7-x}$  no systematic difference between  $S$  or  $S_-$  is found [7].

## References

- [1] P. Varotsos, N. Sarlis, and E. Skordas, Spatiotemporal complexity aspects on the interrelation between Seismic Electric Signals and seismicity, *Practica of Athens Academy*, 76, 294–321, 2001.
- [2] P. A. Varotsos, N. V. Sarlis, and E. S. Skordas, Long-range correlations in the electric signals that precede rupture, *Phys. Rev. E*, 66, 011902 (7), 2002.
- [3] P. A. Varotsos, N. V. Sarlis, and E. S. Skordas, *Natural Time Analysis: The new view of time. Precursory Seismic Electric Signals, Earthquakes and other Complex Time-Series* (Springer-Verlag, Berlin Heidelberg) 2011.
- [4] P. A. Varotsos, N. V. Sarlis, E. S. Skordas, S. Uyeda, and M. Kamogawa, Natural time analysis of critical phenomena, *Proc. Natl. Acad. Sci. USA* 108, 11361–11364, 2011.

- [5] P. A. Varotsos, N. V. Sarlis, H. K. Tanaka and E. S. Skordas, Similarity of fluctuations in correlated systems: The case of seismicity, *Phys. Rev. E* 72, 041103(8), 2005.
- [6] N. V. Sarlis and S.-R. G. Christopoulos, Natural time analysis of the Centennial Earthquake Catalog, *CHAOS* 22, 023123(7), 2012.
- [7] N. V. Sarlis, E. S. Skordas, and P. A. Varotsos, Similarity of fluctuations in systems exhibiting Self-Organized Criticality, *EPL* 96, 28006, 2011.
- [8] P. A. Varotsos, N. V. Sarlis, and E. S. Skordas, Attempt to distinguish electric signals of a dichotomous nature, *Phys. Rev. E*, 68, 031106 (7), 2003.
- [9] P. A. Varotsos, N. V. Sarlis, E. S. Skordas, and M. S. Lazaridou, Entropy in the natural time-domain, *Phys. Rev. E*, 70, 011106(10), 2004.
- [10] P. A. Varotsos, N. V. Sarlis, H. K. Tanaka and E. S. Skordas, Some properties of the entropy in the natural time, *Phys. Rev. E*, 71, 032102(4), 2005.

Dynamics of polymer chains near  
a patterned surface in a slit and in a tube  
– a computer simulation study

A. Sikorski, S. Jaworski, L. Ołdziejewski

*Department of Chemistry, University of Warsaw  
Pasteura 1, 02-093 Warsaw, Poland*

The introduction of surfaces affects most properties of polymer chains. These surfaces can play the role of model nanoparticles or nanotubes. We developed and studied a coarse-grained model of macromolecules near a patterned surface, in a slit and in a tube. A lattice representation of chains was employed and the chains were studied under good solvent conditions. Therefore, the excluded volume was the only interaction between the segments of the chain. The model systems were studied by means of dynamic Monte Carlo simulations with a sampling algorithm based on the local changes of the conformations of the chains. The dependence of the chain structure and mobility on: the width of the slit or the tube, the pattern on the surface, the temperature and on the polymer concentration was studied. The influence of: the chain length, the width of the slit and of the temperature on the frequency of such jumps was also studied. The mobility of the chains was also investigated and the changes in the mechanism of motion were discussed.

## Graphite to graphene oxide conversion and decoration with silver nanoparticles using solar light

N. Todorova, E. C. Vermisoglou, M. Giannouri, T. Giannakopoulou,  
D. Petridis, C. Trapalis

*Institute of Advanced Materials, Physicochemical Processes,  
Nanotechnology and Microelectronics  
National Center for Scientific Research "Demokritos", Athens, 153 10, Greece*

Bare and silver decorated graphene materials were prepared by oxidation of graphite and further reduction/metal deposition procedures. Three types of graphite, namely flakes, powder and expandable graphite were used as starting materials. The oxidation was performed by applying both modified Staudenmayer and Hummers methods. The level of oxidation depending on the pristine graphite and the preparation route was investigated. High temperature annealing in vacuum and fast microwave irradiation were performed to obtain reduced graphite oxide. Also, solar light irradiation was employed for simultaneous GO reduction and Ag nanoparticles deposition on the graphitic materials using  $\text{AgNO}_3$  as the metal precursor.

The structural transitions from graphite to GO as well as the Ag nanoparticles deposition were examined by the X-Ray Diffraction analysis. The treatment of smaller graphite particles by the Hummers method resulted in a high level of oxidation of the initial material after a single oxidation cycle. The photo-reduction of the GO upon solar light irradiation was also recorded and enhancement by addition of  $\text{AgNO}_3$  was observed. The average particle size of Ag in the composite materials was found to be  $\sim 40$  nm.

The FTIR and UV-Vis spectroscopy results confirmed the GO reduction under solar irradiation and its acceleration in the presence of Ag. The SEM analysis revealed that the microwave treatment resulted in exfoliation of the initial graphite and the prepared graphite oxide. The element mapping and EDAX analysis confirmed the Ag deposition in the composite materials. Although well dispersed, the Ag exhibited a tendency for agglomeration in clusters up to 200 nm.

It is expected that the prepared Graphene oxide/Silver nanocomposite materials could find promising application in the fields of catalysis, plasmonic photocatalysis, biosensors and memory devices.

# Comparison of magnetic characterizations of nanoparticles obtained by SQUID magnetometry and FMR

J. Typek<sup>1</sup>, N. Guskos<sup>1,2</sup>, K. Wardal<sup>1</sup>, G. Żolnierkiewicz<sup>1</sup>

<sup>1</sup>*Institute of Physics, West Pomeranian University of Technology  
Al. Piastów 48, 70-311 Szczecin, Poland*

<sup>2</sup>*Department of Solid State Physics, University of Athens  
Panepistimiopolis, 15 784 Zografou, Athens, Greece*

A comparison will be made between the magnetic characterization of nanoparticles using the techniques of SQUID (superconducting quantum interference device) dc magnetometry and ferromagnetic resonance (FMR). A wide spectrum of different magnetic nanoparticles were studied, including  $\text{ZnFe}_2\text{O}_4$  [1],  $\alpha\text{-Fe}$  [2],  $\gamma\text{-Fe}_2\text{O}_3$  (maghemite) [3],  $\text{Fe}_3\text{O}_4$  (magnetite) [4],  $\text{Fe}_3\text{C}$  (cementite) [5], Co [6], Ni [7], TiC [8]. The studied magnetic nanoparticles were in a concentrated form, forming large agglomerates of different sizes, or were dispersed in non-magnetic matrices (multiblock copolymers, cements, glues, waxes, paraffin, graphite).

The basic SQUID magnetometry characterization was performed by isothermal measurements under the applied magnetic field using the zero-field-cooling (ZFC) and field-cooling (FC) methods. The FMR studies were carried out on a Bruker E 500 spectrometer operating in X-band in the 4–300 K range. These two techniques could provide complementary results which when properly interpreted allow gaining a broader range of information about the studied spin systems. Particular attention will be paid to the determination of these magnetic parameters (blocking temperatures, magnetization saturation, anisotropy fields) that could be calculated independently from the experimental results obtained by using both the techniques.

## References

- [1] Guskos N, Glenis S, Żolnierkiewicz G, Typek J, Berczynski P, Guskos A, Sibera D, and Narkiewicz U, (2012) *Appl. Phys. Lett.* **100** 122403
- [2] Helminiak A, Arabczyk W, Żolnierkiewicz G, Guskos N, Typek J, (2011) *Rev. Adv. Mater. Sci.* **29** 166
- [3] Guskos N, Glenis S, Likodimos V, Typek J, Maryniak M, Roslaniec Z, Kwiatkowska M, Baran M, Szymczak R, Petridis D, (2006) *J. Appl. Phys.* **99** 084307
- [4] Bodziony T, Guskos N, Typek J, Roslaniec Z, Narkiewicz U, Kwiatkowska M, Maryniak M, (2004) *Rev. Adv. Mater. Sci.* **8** 86
- [5] Guskos N, Typek J, Maryniak M, Narkiewicz U, Kucharewicz I, Wrobel R, (2005) *Mater. Sci. - Poland* **23** 1001
- [6] Guskos N, Typek J, Maryniak M, Żolnierkiewicz G, Podsiadly M, Arabczyk W, Lenzion-Bielun Z and Narkiewicz U, (2006) *Mater. Sci. - Poland* **24** 1095
- [7] Guskos N, Maryniak M, Typek J, Podsiadly M, Narkiewicz U, Senderek E, and Roslaniec Z, (2009) *J. Non-Cryst. Solids* **355** 1400
- [8] Guskos N, Typek J, Bodziony T, Żolnierkiewicz G, Maryniak M, Biedunkiewicz A, (2009) *J. Alloy. Compd.* **470** 51

## Materials of anomalous mechanical properties

K. W. Wojciechowski<sup>1</sup>, A. A. Poźniak<sup>2</sup>

<sup>1</sup>*Institute of Molecular Physics, Polish Academy of Sciences  
M. Smoluchowskiego 17/19, 60-179 Poznań, Poland*

<sup>2</sup>*Institute of Physics, Poznań University of Technology  
Nieszawska 13A, 60-965 Poznań, Poland*

The recent progress in studies of systems exhibiting negative Poisson's ratio (known as auxetics) and/or negative compressibility will be discussed in this lecture. The results of theoretical modeling and computer simulations will be presented with emphasis on particle methods and finite element methods.

### **Acknowledgements**

This work was supported by grant NN202261438 of the Polish Ministry of Science and Education. Some calculations were performed at the Poznań Computing and Networking Center (PCSS).

## Filling porous silicate glasses with $\text{Fe}_3\text{O}_4$ magnetic nanoparticles

B. Zapotoczny<sup>1</sup>, M. R. Dudek<sup>1</sup>, N. Gouskos<sup>2,3</sup>, J. J. Koziół<sup>4</sup>,  
B. V. Padlyak<sup>1,5</sup>, E. Rysiakiewicz-Pasek<sup>6</sup>

<sup>1</sup>*Institute of Physics, University of Zielona Góra  
Szafrana 4a, 65-069 Zielona Góra, Poland*

<sup>2</sup>*Department of Solid State Physics, University of Athens  
Panepistimiopolis, 15 784 Zografou, Athens, Greece*

<sup>3</sup>*Institute of Physics, West Pomeranian University of Technology  
Al. Piastów 17, 70-310 Szczecin, Poland*

<sup>4</sup>*Faculty of Biological Sciences, University of Zielona Góra  
Szafrana 1, 65-516 Zielona Góra, Poland*

<sup>5</sup>*Sector of Spectroscopy, Institute of Physical Optics  
Dragomanova 23, 79-005 Lviv, Ukraine*

<sup>6</sup>*Institute of Physics, Wrocław University of Technology  
Wyb. Wyspiańskiego 27, 50-370 Wrocław, Poland*

The results of the research on new magnetic materials for biomedical applications are discussed. The materials are nanoporous silicate glasses with magnetic fillers. The magnetic fillers are bare magnetite nanoparticles ( $\text{Fe}_3\text{O}_4$ ) to ensure the smallest number of components for subsequent removal from the body. The glasses were obtained as a leaching product from one sodium-boro-silicate glass with the following chemical composition: 90–91%  $\text{SiO}_2$ , 8.3–8.7%  $\text{B}_2\text{O}_3$ , 0.3–0.6%  $\text{Na}_2\text{O}$  (% mol). The  $\text{Fe}_3\text{O}_4$  nanoparticles were synthesized according to Massart's method [1] and their diameter did not exceed 20 nm. Two experimental techniques were compared. In the first one [2] the glass samples were immersed in an aqueous suspension of magnetite nanoparticles ( $\text{Fe}_3\text{O}_4$ ) for a given value of pH for about 48 hours. In this case the nanoparticles filled the pores as a result of diffusion from an aqueous suspension of nanoparticles to the glass pores. The filling process strongly depended on the pH value. The second technique was synthesis of magnetic nanoparticles directly in the pores of silica glasses. The magnetic properties of these materials were investigated using the ferromagnetic resonance method (FMR). The obtained results are supported by computer simulations of ferromagnetic resonance (FMR) for a cluster of  $N$  magnetic nanoparticles locked in a porous medium with the help of the models discussed in [4].

### References

- [1] R. Massart, *Preparation of Aqueous Magnetic Liquids in Alkaline and Acidic Media*, IEEE T. Magn. **17** (2), 1247 (1981).
- [2] B. Zapotoczny, M. R. Dudek, N. Guskos, J. J. Koziół, B. V. Padlyak, M. Kośmider, E. Rysiakiewicz-Pasek, *FMR study of the porous silicate glasses with  $\text{Fe}_3\text{O}_4$  magnetic nanoparticles fillers*, Journal of Nanomaterials (2012).

- [3] M. R. Dudek, N. Guskos, E. Senderek, Z. Roslaniec *Temperature dependence of the FMR absorption lines in viscoelastic magnetic materials*, Journal of Alloys and Compounds 504, 289-295 (2010).
- [4] M. R. Dudek, N. Guskos, M. Kosmider, *Thermal Effects on the Ferromagnetic Resonance in Polymer Composites with Magnetic Nanoparticles Fillers* in Smart Nanoparticles Technology, pp. 373-386, Edited by Abbass A. Hashim, InTech, April 2012.

# A modified Langmuir-Schaefer approach to synthesis of highly-ordered clay/carbon nanotube hybrids

P. Zygouri<sup>1</sup>, P. Stathi<sup>2</sup>, T. Tsoufis<sup>2</sup>, A. Kouloumpis<sup>1</sup>, D. Gournis<sup>1</sup>,  
P. Rudolf<sup>2</sup>

<sup>1</sup>*Department of Materials Science and Engineering, University of Ioannina  
45100 Ioannina, Greece*

<sup>2</sup>*Zernike Institute for Advanced Materials, University of Groningen  
Nijenborgh 4, 9747AG Groningen, the Netherlands*

Much of the research effort concerning the nanoscopic properties of layered materials focuses on their use as building blocks for the development of new hybrid nanostructures with well-defined dimensions and behavior. The objective of this work is the synthesis of a new type of clay-based hybrid materials for application in gas storage/separation, heterogeneous catalysis and sensing: nanometer-sized clay platelets are sandwiched with carbon nanotubes through layer-by-layer deposition and intercalation chemistry to yield novel pillared carbon nanotube-clay structures. A bottom-up approach was applied for the production of hybrid materials where smectite clay nanoplatelets act as the structure-directing interface and reaction media. This method, based on combining self-assembly with the Langmuir Schaefer technique [1], uses the clay nanosheets as a template for the grafting functionalized carbon nanotubes in a bi-dimensional array, and allows for perfect layer-by-layer growth with control at the molecular level. Initially, CNTs were functionalized with phenol groups via 1,3-dipolar cycloaddition in a single step using commercially available reagents [2]. Sidewall functionalization provided stable dispersions of CNTs in water and other polar solvents. A dilute water solution of clay was used as a subphase on the Langmuir-Blodgett deposition system while an appropriate amino surfactant (that binds electrostatically to the clay surface) was applied for the formation of hybridized organo-clay. After the horizontal lift of a hydrophobic substrate, a surface modification of the clay platelets was performed by bringing the surface of the transferred Langmuir film in contact with a second amino surfactant solution (capable of interacting strongly with the functionalized nanotubes). In the final step, the hybrid organo-clay film was lowered in the solution of the functionalized CNTs. Multilayer films were constructed by repeating this procedure. Hybrid clay/CNT thin films deposited on various hydrophobic substrates were characterized by X-ray diffraction, FTIR, Raman and X-ray photoelectron spectroscopies as well as Atomic Force Microscopy.

## References

- [1] Toma L. M., Prinsen E. B., Gournis D. and Rudolf P. 2010 *Phys. Chem. Chem. Phys.* **12** 12188
- [2] Gengler R. Y. N., Gournis D., Aimon A. H., Toma L. M. and Rudolf P. 2012 *Chem. Eur. J.* in press (doi: 10.1002/chem.201103528)
- [3] Georgakilas V., Bourlinos A., Gournis D., Tsoufis T., Trapalis C., Mateo-Alonso A. and Prato M. 2008 *J. Am. Chem. Soc.* **130** 8733



# POSTERS



# Comparative study of methods for synthesizing mixed nanoferrites and of their magnetic properties

A. Amirabadizadeh

*Department of Physics, Faculty of Science  
University of Birjand  
Birjand, Iran*

The study of nanoferrites is of great importance owing to the widespread applications of these magnetic nanoparticles in biomedicine, biotechnology, engineering and materials science.

Ferrite preparation is the objective of a large number of studies, yet it remains an open problem. The question is “how to obtain better performance of ferrite material?”

In the present investigation an attempt has been made to comparatively study different methods for the synthesis of the nanostructured mixed oxide ferrite powders (M-Zn nanoferrite, M = Mn and Ni). This review focuses on the co-precipitation, sol-gel and reverse micelles methods. These methods are briefly reviewed, and the particle size and magnetic properties of nanoparticles prepared by the aforementioned methods are compared.

# Nanomechanical properties of metallic fcc nanorods from molecular simulations with the Sutton-Chen force field

M. Białoskórski<sup>1</sup>, J. Rybicki<sup>1,2,3</sup>

<sup>1</sup>*TASK Computer Center, Gdansk University of Technology  
Narutowicza 11/12, 80-233 Gdansk, Poland*

<sup>2</sup>*Department of Solid State Physics, Gdansk University of Technology  
Narutowicza 11/12, 80-233 Gdansk, Poland*

<sup>3</sup>*Institute of Mechatronics, Nanotechnology and Vacuum Techniques  
Koszalin University of Technology  
Raclawicka 5-17, 75-620 Koszalin, Poland*

Basic elastic constants (Young's modulus, Poisson coefficient, shear modulus) were determined for several monocrystalline metallic (Ni, Cu, Pt, Au) nanorods using molecular dynamics with the Sutton-Chen force field. Stress-strain curves were also calculated and discussed. The conclusions are as follows.

The conducted systematic studies of monocrystalline nanorods showed the effect of the direction of the load on the mechanical properties, while the corresponding effect of the nanorod diameter was observed only for rods with a diameter below 8 lattice constants. The analysis of the obtained results shows that Young's modulus is highest measured in the [111] direction and remains invariant when the direction of the load is reversed. Its value is lowest when measured in the [001] direction, in this case it is smaller by a factor of 20 for compression compared with stretching. For the [011] direction it is 50 times higher for compression compared with stretching. The values of Poisson's ratio and shear modulus are the highest for the load in the [001] direction, and the lowest for the [111] direction. Beyond the yield point slips were observed in the planes of densest packing {111}, regardless of the direction of the load, and they always originated from the outer surface of the nanorod.

The described dependence of the mechanical properties of nanostructures on the type of load (compression vs. stretching), not considered in the literature, still requires confirmation by comparison with experiment and with more accurate (ab initio) computational approaches.

The obtained results reveal that coming up with a correct nanomechanical model requires the use of different material constants depending on the mechanics of the system which they describe. As in the case of macroscopic systems, material constants offer a correct description only for strains below 2%. For strains in the order of  $\pm 80\%$  of the strain required to break the nanostructure, it is sufficient to use a quadratic function to describe the stress-strain dependence. In the entire range of elastic strains, this dependence can be described by a cubic polynomial (with an uncertainty below 8%).

The presented analysis showed that the approaches used in the theory of elasticity and strength of materials can be used for nanostructures comprising more than 1000 atoms. However, all the characteristics of the materials should and may be obtained computationally using MD. A description of the behaviour of a nanostructure under load may be obtained by strength of materials methods, while for complicated cases the finite element method can be employed whereby it becomes possible to create models whose sizes exceed those admitted by particle methods.

**Acknowledgements**

This work was supported by grant N519 024 32/3053 of the Polish Ministry of Science and Education.

# Long-lasting solubilisation of multi-walled carbon nanotubes by synthetic humic acids

E. Bletsa<sup>1,2</sup>, Y. Deligiannakis<sup>1</sup>, D. Gournis<sup>2</sup>

<sup>1</sup>*Laboratory of Physical Chemistry of Materials & Environment  
Department of Environmental and Natural Resources Management  
University of Western Greece  
Seferi 2, 30100 Agrinio, Greece*

<sup>2</sup>*Department of Materials Science and Engineering, University of Ioannina  
45100 Ioannina, Greece*

A carbon nanotube (CNT), a form of elementary carbon, is composed of graphitic sheets rolled into closed concentric cylinders with a diameter of the order of nanometers and a length of the order of micrometers. CNTs have received great interest due to their unique properties and a wide scope of possible applications. However, a major barrier for utilization of CNTs is their poor solubility and dispersability both in aqueous and polar solvents. CNTs are extremely hydrophobic and prone to aggregation and deposition in water due to strong inter-nanotube van der Waals forces [1]. Sonication plays a key role in the stabilization of CNT suspensions by gradually disentangling CNTs from their aggregates and bundles. As the production and applications of CNTs expand, the introduction of CNTs into the environment increases continuously. Natural surface-active materials, such as humic acids (HA) are widely distributed in the environment. They may adsorb onto individual CNTs, and thus alter their surface physicochemical properties and enhance their stabilization in water [2]. Thus, monitoring and controlling the CNT-HA interaction is of key importance. In the present work we present a study of the solubilization effect of well characterized synthetic Humic Acids on Multi-Walled CNTs (MWCNTs) with Attenuated Total Reflection (ATR) FTIR spectroscopy. A well characterised Humic Acid Like Polycondensate (HALP) produced with no use of a catalyst [3] shows a remarkable capability for solubilisation of – otherwise water-insoluble – MWCNTs. ATR-FTIR spectroscopy was used to study the molecular interactions between the HALP (as well as the standard IHSS Leonardite HA as a reference) with MWCNTs at various pH values. The data show that CNTs cause specific changes in the spectral features of both HALP and LHA. These spectral changes are sensitive to pH, indicating that deprotonable groups of humics are involved in the interaction with MWCNTs. Finally, while MWCNTs are not soluble in water, the presence of HALP forms non-precipitating colloid suspensions which are practically unaltered for at least two weeks.

## References

- [1] Pang Y., Xu G., Yuan S., Tan Y. and He F. 2009 *Colloid Surface* **350** 101.
- [2] Lin D. and Xing B. 2008 *Environ. Sci. Technol.* **42** 5917.
- [3] Giannakopoulos E., Drosos M. and Deligiannakis Y. 2009 *J. Colloid Interf. Sci.* **336** 59.

---

# Anomalous mechanical behaviour from metamaterials with magnetic components

R. Caruana-Gauci<sup>1</sup>, M. R. Dudek<sup>2</sup>, K. W. Wojciechowski<sup>3</sup>,  
J. N. Grima<sup>1,4</sup>

<sup>1</sup>*Metamaterials Unit, Faculty of Science, University of Malta  
Msida MSD 2080, Malta*

<sup>2</sup>*Institute of Physics, Zielona Góra University  
65-069 Zielona Góra, Poland*

<sup>3</sup>*Institute of Molecular Physics, Polish Academy of Sciences  
Smoluchowskiego 17, 60-179, Poznań, Poland*

<sup>4</sup>*Department of Chemistry, Faculty of Science, University of Malta  
Msida MSD 2080, Malta*

Systems which exhibit anomalous mechanical behaviour such as negative Poisson's ratio or negative compressibility are typically studied under the conditions of externally applied mechanical forces or imposed displacements. Here we consider mechanical systems having magnetic components which are being deformed by forces which are not purely mechanical. In particular, we present some of our results obtained through computer simulations, analytical modelling and experiments. These were carried out in an attempt to assess if magnetic systems have a potential to exhibit some anomalous mechanical properties.

It was found that localized magnetic fields can affect the microscopic and the macroscopic behaviour of the system what results in change of their mechanical properties. Depending on the design of such systems, the anomalous mechanical properties which arise can either be always present or they can appear in the presence of an externally applied magnetic field.

Apart from interesting anomalous mechanical properties which are observed in such systems, like e.g. negative Poisson's ratio, negative compressibility and moduli dependent on the relative position and orientation of the magnets within the structure, other properties were observed, including negative rotational stiffness and other electromagnetic effects such as, e.g., induced electric currents.

## **Acknowledgements**

The support of the University of Malta as well as the support of the Univeristy of Zielona Góra is gratefully acknowledged. Joseph N. Grima and Krzysztof W. Wojciechowski acknowledge the support of the project POKL.04.01.01-00-041/09-00 which has awarded them visiting professorships.

# On obtaining negative linear compressibility through elongation of the ribs

R. Caruana-Gauci<sup>1</sup>, K. W. Wojciechowski<sup>2</sup>, J. N. Grima<sup>1,3</sup>

<sup>1</sup>*Metamaterials Unit, Faculty of Science, University of Malta  
Msida MSD 2080, Malta*

<sup>2</sup>*Institute of Molecular Physics, Polish Academy of Sciences  
Smoluchowskiego 17, 60-179, Poznań, Poland*

<sup>3</sup>*Department of Chemistry, Faculty of Science, University of Malta  
Msida MSD 2080, Malta*

Materials and structures which expand in at least one direction when hydrostatically compressed are termed to exhibit negative linear compressibility. Several materials have been reported in literature to exhibit such a property including methanol monohydrate, caesium dihydrogen phosphate and lanthanum niobate. Several model systems have been proposed to exhibit negative linear compressibility such as the honeycomb, wine-rack models and tetragonal beam structures. It was previously shown that hexagonal honeycombs and related systems can exhibit negative linear compressibility when they have a high positive Poisson's ratio and deform through a change in the angle between the ribs (see Fig. 1a). Here we extend this early and preliminary study and show that negative compressibility is also permissible in some specific cases for re-entrant honeycomb-like systems constructed from ribs with different stiffnesses deforming solely through changes in length of the ribs (an idealised stretching mechanism) (see Fig. 1b). Practical requirements for this effect to be manifested are discussed in detail.

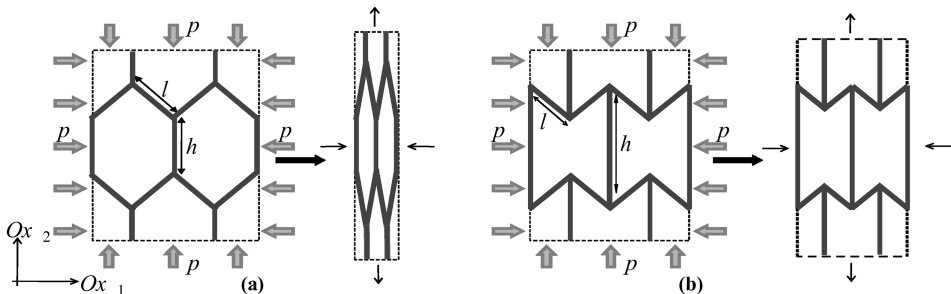


Figure 1: The (a) hexagonal honeycomb deforming through the idealised hinging mechanism and the proposed (b) re-entrant honeycomb deforming through the idealised stretching mechanism exhibit negative linear compressibility when placed under a hydrostatic pressure  $p$ .

**Acknowledgements**

The support of the Malta Council of Science and Technology through their national R&I programme as well as the support of the University of Malta is gratefully acknowledged. Krzysztof W. Wojciechowski acknowledges the support of the project POKL.04.01.01-00-041/09-00 which has awarded him a visiting professorship.

## Modelling of auxetic crystals

R. Cauchi<sup>1</sup>, K. M. Azzopardi<sup>1</sup>, R. Gatt<sup>2</sup>, D. Attard<sup>2</sup>,  
J. Rybicki<sup>3</sup>, J. N. Grima<sup>1,2</sup>

<sup>1</sup>*Department of Chemistry, Faculty of Science, University of Malta  
Msida MSD 2080, Malta*

<sup>2</sup>*Metamaterials Unit, Faculty of Science, University of Malta  
Msida MSD 2080, Malta*

<sup>3</sup>*Department of Solid State Physics, Gdansk University of Technology  
Narutowicza 11/12, 80-233 Gdansk, Poland*

This paper presents preliminary modelling work on crystalline systems which have a potential to exhibit auxetic behaviour in some crystallographic planes for loading in particular directions. Such property is very important in view of the many potential applications of auxetic and related systems such as smart nanofiltration.

### **Acknowledgements**

This research work is partly funded by the University of Malta, Malta Council for Science and Technology and by grants awarded to Reuben Cauchi and Keith M. Azzopardi through the Strategic Educational Pathways Scholarship – Malta. These scholarships are part-financed by the European Union – European Social Fund (ESF) under Operational Programme II – Cohesion Policy 2007–2013, “Empowering People for More Jobs and a Better Quality of Life”

# Dynamics of NO molecules near wall of fullerenols $C_{60}(OH)_{24}$ in aqueous solution – MD study

A. Dawid, K. Górny, Z. Gburski

*Institute of Physics, University of Silesia  
Uniwersytecka 4, 40-007, Katowice, Poland*

The dynamics of nitric oxide molecules near the wall of polyhydroxylated fullerene derivative, fulleranol  $C_{60}(OH)_{24}$  (inset of Fig. 1) was simulated by the MD method. The study was motivated by the expected diverse biological applications of water soluble fullerenols. The nitric oxide is known as one of the most important signaling molecules in the mammal's body. Both in vitro and in vivo studies have shown that fullerenols can be potential antioxidative agents and free radical scavengers in biological systems [1]. Computer simulation calculations have shown that a single  $C_{60}(OH)_{24}$  molecule is able to attract small numbers of nitric oxide molecules in an aqueous solution [2]. In the current work we simulated the dynamics of NO molecules near the wall of fulleranol molecules (Fig. 1). The simulations were fully atomistic with intra- and intermolecular potentials. The slight scavenging of NO molecules on

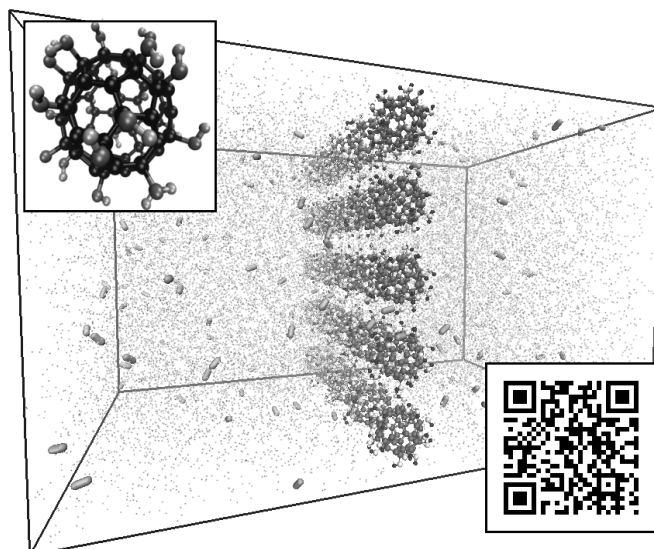


Figure 1: Instantaneous configuration of the studied system (water molecules are not shown for clarity). The inset shows a modeled fulleranol molecule and the QR code containing the simulation movie address [http://www.youtube.com/watch?v=CMNR\\_cL1YXs](http://www.youtube.com/watch?v=CMNR_cL1YXs)

the wall of fullerenols was tested by calculating the radial distribution functions, the static structure factor related to the neutron scattering experiment and the mean square displacement functions.

## References

- [1] S. Trajkovic, S. Dobric, V. Jacevic, et al, *Colloids and Surfaces B: Biointerfaces* 58 (2007) pp. 39–43
- [2] A. Dawid, K. Górny and Z. Gburski, *Nitric Oxide – Biology and Chemistry* 25 (2011) 4 pp: 373–380

---

# Non-Debye dipolar relaxation of ethylene glycol embedded in ZSM-5 zeolite host matrix – computer simulation study

Z. Dendzik, K. Górny, Z. Gburski

*Institute of Physics, University of Silesia  
Uniwersytecka 4, 40-007 Katowice, Poland*

Studying the behavior of molecules in nanoscale confinement is particularly important to understand many processes in biology - such as protein transport in biomembranes and other processes taking place in living cells - as well as in geology, materials sciences and many other fields [1–3]. Molecular systems confined in a variety of nanoporous media exhibit interesting structural and dynamical properties which can be investigated experimentally, theoretically and by means of computer simulation methods [4–6]. We performed fully atomistic molecular dynamics simulations of ethylene glycol confined inside ZSM-5 zeolite in order to study the effect of the spatial confinement and interaction between the embedded molecules and the host channels internal surface on the system dynamics. We found the change in the thermal activation to be a characteristic as well as considerable deviation of the dynamics in this system from the almost purely exponential relaxation observed in the bulk ethylene glycol liquid.

## References

- [1] D. Fu, A. Libson, L. J. W. Miercke, C. Weitzman, P. Nollert, J. Krucinski, R. M. Stroud, *Science* 290, 481 (2000).
- [2] K. Morishige, K. Kawano, *J. Chem. Phys.* 110, 4867 (1999).
- [3] U. Raviv, P. Laurat, J. Klein, *Nature* 413, 51 (2001).
- [4] Z. Dendzik, K. Górny, Z. Gburski, *J. Phys.: Condens. Matter* 21, 425101 (2009).
- [5] S. Gautam, V. K. Sharma, S. Mitra, S. L. Chaplot, R. Mukhopadhyay, *Chem. Phys. Lett.* 501, 345 (2011).
- [6] K. Górny, Z. Dendzik, P. Raczynski, Z. Gburski, *Solid State Comm.* 152, 8 (2012).

## Hexagonal auxetics

R. V. Goldstein, V. A. Gorodtsov, D. S. Lisovenko

*A. Yu. Ishlinsky Institute for Problems in Mechanics RAS  
 Prosp. Vernadskogo 101-1, 119526 Moscow, Russia*

The mechanical properties of anisotropic materials depend on the orientation of the investigated samples. In particular, the elastic properties of crystals upon uniaxial tension and shear such as Young's modulus  $E(\mathbf{n})$ , Poisson's ratio  $\nu(\mathbf{n}, \mathbf{m})$ , and shear modulus  $G(\mathbf{n}, \mathbf{m})$  depend on the mutually orthogonal unit vectors  $\mathbf{n}$  and  $\mathbf{m}$  that characterize the crystal strain direction. The general form of these dependences for arbitrary anisotropic materials is well-known:

$$\frac{1}{E(\mathbf{n})} = s_{ijkl}n_i n_j n_k n_l, \quad \frac{\nu(\mathbf{n}, \mathbf{m})}{E(\mathbf{n})} = -s_{ijkl}n_i n_j m_k m_l,$$

$$\frac{1}{4G(\mathbf{n}, \mathbf{m})} = s_{ijkl}n_i m_j n_k m_l.$$

Below, instead of fourth-order elastic-moduli tensors  $s_{ijkl}$ , we use the matrix compliances  $s_{mn}$ . We proceed from the mentioned crystal orientation parameterization by components of vectors  $\mathbf{n}$  and  $\mathbf{m}$  to the use of three Euler angles  $\varphi$ ,  $\theta$ , and  $\psi$ .

In the special case of hexagonal crystals, the number of different matrix elastic coefficients decreases to five ( $s_{11}$ ,  $s_{12}$ ,  $s_{13}$ ,  $s_{33}$ , and  $s_{44}$ ). The dependence of Young's modulus, Poisson's ratio, and shear modulus on these coefficients and the Euler angles can be presented in the form:

$$\frac{1}{s_{11}E} = 1 + (\Pi_1 - \Pi_{01} \sin^2 \theta) \cos^2 \theta, \quad (1)$$

$$-\frac{\nu}{s_{13}E} = 1 + (\Pi_2 \sin^2 \psi + \Pi_{02} \cos^2 \theta \cos^2 \psi) \sin^2 \theta, \quad (2)$$

$$\frac{1}{s_{44}G} = 1 + (\Pi_3 \sin^2 \psi + 4\Pi_{03} \cos^2 \theta \cos^2 \psi) \sin^2 \theta, \quad (3)$$

$$\Pi_{01} \equiv \frac{\delta}{s_{11}}, \quad \Pi_{02} \equiv \frac{\delta}{s_{13}}, \quad \Pi_{03} \equiv \frac{\delta}{s_{44}},$$

$$\Pi_1 \equiv \frac{s_{33} - s_{11}}{s_{11}}, \quad \Pi_2 \equiv \frac{s_{12} - s_{13}}{s_{13}}, \quad \Pi_3 \equiv \frac{2s_{11} - 2s_{12} - s_{44}}{s_{44}},$$

$$\delta \equiv s_{11} + s_{33} - 2s_{13} - s_{44}.$$

Here, the dimensionless elastic moduli appear dependent on the corresponding pairs of dimensionless combinations of the matrix compliances and the Euler angles. Young's modulus depends on one Euler angle  $\theta$  and does not depend on the other two angles,

while Poisson's ratio and the shear modulus appear to be dependent on the two Euler angles  $\theta$  and  $\psi$  and independent of the third angle  $\varphi$ . The dimensionless complexes  $\Pi_{0n}$  and  $\Pi_n$  and the dimensional parameter  $\delta$  are characteristics of the degree of anisotropy of hexagonal crystals. They vanish in the isotropic medium limit.

Very few from among hexagonal crystals are auxetics. Their number is especially small compared with the number of cubic auxetics [1]. The boundary of auxeticity of hexagonal auxetics at which Poisson's ratio vanishes is described, according to (2), by the curve equation:

$$(\Pi_2 \sin^2 \psi + \Pi_{02} \cos^2 \theta \cos^2 \psi) \sin^2 \theta = -1. \quad (4)$$

Using the experimental data for the compliances of hexagonal crystals from the Landolt-Börstein reference book [2], six hexagonal auxetics (MoS<sub>2</sub>, C<sub>7</sub>H<sub>12</sub>, Zn, BeCu (2.4 at.% Cu), TiB<sub>2</sub>, Be) were revealed. We plotted auxetical curves  $\nu(\theta, \psi) = 0$  (4) for these crystals. These curves for hexagonal crystal auxetics MoS<sub>2</sub> and Zn, on the one hand, and the C<sub>7</sub>H<sub>12</sub>, BeCu, TiB<sub>2</sub>, and Be crystals, on the other hand, are qualitatively different. For the crystals of the first type, the curves represent single ovals, while the auxetical curve of the C<sub>7</sub>H<sub>12</sub>, BeCu, TiB<sub>2</sub> and Be crystals consists of a pair of separate ovals cut by the abscissa axis and the line  $\psi = \pi$  parallel thereto that are identified by virtue of angular periodicity. The smallest negative value of Poisson's ratio  $\nu_{min} = -0.282$  is attained for the molybdenum disulfide MoS<sub>2</sub> single crystal upon its orientation  $\theta = \psi = \pi/2$ . It should be noted that the angular dependence of Poisson's ratio of beryllium and its alloy varies slightly near zero. For hexagonal auxetics, the extreme values of Poisson's ratio were determined. The simple extreme values are  $-s_{13}/s_{33}$  at  $\theta = 0$  and the arbitrary angle  $\psi$ ,  $-s_{13}/s_{11}$  at the points  $\theta = \pi/2$ ,  $\psi = 0$  and  $-s_{12}/s_{11}$  at the points  $\theta = \psi = \pi/2$ . The existence of other extreme values is possible only upon certain limitations put on the dimensionless complexes of compliances, i.e., for a few specific hexagonal crystals.

Extreme, always positive, values of Young's modulus are consistent with the vanishing of the angular variable derivative of expression (1). Two extreme values,  $1/s_{33}$  and  $1/s_{11}$ , are attained at  $\theta = 0$  and  $\theta = \pi/2$ , respectively. The extreme value  $E = (1/s_{11}) \cdot (4\Pi_{01}) / (4\Pi_{01} - (\Pi_1 - \Pi_{01})^2)$  can also be attained at condition  $0 < (\Pi_1 - \Pi_{01}) / (4\Pi_{01}) < 1$ . The greatest variability of Young's modulus is achieved in MoS<sub>2</sub> (from 44.9 to 209 GPa) and Zn (from 36.1 to 126 GPa).

The extreme values of the shear modulus and their positions on the plane of angles  $\theta$  and  $\psi$  are determined by formula (3). The extreme value  $1/s_{44}$  is attained on the line  $\theta = 0$  at any angles  $\psi$  and at the point  $\theta = \pi/2$ ,  $\psi = 0$ . The extreme value of the shear modulus  $(1 + \Pi_{03})^{-1}/s_{44}$  is attained at the point  $\theta = \pi/4$ ,  $\psi = 0$ . At the extreme point  $\theta = \psi = \pi/2$ , the shear modulus acquires the value  $1/s_{66} = 1/(2s_{11} - 2s_{12})$ . The existence of other extreme values is possible only upon certain limitations put on the dimensionless complexes of compliances. The greatest variability of the shear modulus is achieved in MoS<sub>2</sub> (from 18.6 to 146 GPa) and Zn (from 20 to 70.4 GPa).

An analysis of the experimental data shows relatively small changes in the Young and shear moduli at the change in orientation of beryllium and its alloys with copper. This ensures a very small change in the size of the samples of these materials, which makes it possible to use beryllium and its alloys in fabrication of products with high stability of dimensions and hardness, such as gyroscopes, mirrors, and lenses.

Using a simple analysis, we showed that auxetic properties do not appear on

averaging over the transverse directions separately, while a global averaging over all orientations of the uniaxially loaded crystal produces a positive Poisson's ratio. The globally calculated Poisson's ratios are 0.21 for MoS<sub>2</sub>, 0.44 for C<sub>7</sub>H<sub>12</sub>, 0.26 for Zn, 0.32 for TiB<sub>2</sub>, 0.03 for Be and BeCu. Note that global Poisson's ratios of Be and BeCu crystals are close to zero.

### **Acknowledgements**

This work was performed in the framework of the Program of Basic Research of the Presidium of the Russian Academy of Sciences no. 25 and Grant MK-565.2012.1 (D.S.L.).

### **References**

- [1] Goldstein R. V., Gorodtsov V. A. and Lisovenko D. S. 2011 *Doklady Physics* **56** (7) 399
- [2] Landolt-Börstein – Group III 1992 *Condensed Matter*, Springer

---

## Study of magnetic properties of $\text{ZnFe}_2\text{O}_4$ nanoparticles at different concentrations of FeO in ZnO matrix

N. Gouskos<sup>1,2</sup>, S. Glenis<sup>1</sup>, G. Żolnierkiewicz<sup>2</sup>, J. Typek<sup>2</sup>,  
P. Berczyński<sup>2</sup>, A. Guskos<sup>2</sup>, K. Wardal<sup>2</sup>, D. Sibera<sup>3</sup>,  
U. Narkiewicz<sup>3</sup>, Z. Lenzion-Bieluń<sup>3</sup>, W. Lojkowski<sup>4</sup>

<sup>1</sup>*Department of Solid State Physics, Faculty of Physics, University of Athens  
Panepistimiopolis, 15 784 Zografou, Athens, Greece*

<sup>2</sup>*Institute of Physics, Faculty of Mechanical Engineering and Mechanics  
West Pomeranian University of Technology  
Al. Piastów 48, 70-311 Szczecin, Poland*

<sup>3</sup>*Institute of Chemical and Environmental Engineering  
West Pomeranian University of Technology  
Al. Piastów 17, 70-310 Szczecin, Poland*

<sup>4</sup>*Institute of High Pressure Physics  
Sokolowska 29/37, 01-142 Warszawa, Poland*

Three samples of nanocrystalline zinc oxide doped with different concentrations of iron oxide (20, 30 and 40 wt.%) were prepared by the wet chemical method. The samples were characterized by X-ray diffraction and scanning electron microscopy and showed growth of  $\text{ZnFe}_2\text{O}_4$  nanocrystallites below 10 nm in size within the ZnO matrix in a highly agglomerated structure. The temperature measurements of the dc magnetization and the ferromagnetic resonance (FMR) signal from liquid helium to room temperature were taken to investigate the magnetic properties of the studied samples. The FMR spectra of the  $\text{ZnFe}_2\text{O}_4$  nanoparticles showed very interesting behavior at different temperatures. The temperature dependence of dc magnetization registered at the applied magnetic field close to the resonance field in the FMR experiment displayed a transition from ferromagnetic to antiferromagnetic interaction in the correlated spin system at about 200 K. At this temperature the amplitude of the FMR resonance line reached a maximum for the three investigated samples. The blocking temperature determined from the dc magnetization measurements fell within in the 26–28 K range and the FMR signal showed some anomaly in this same range.

Pressure study of FMR spectra of 0.1% Ni  
and 0.1%  $\gamma$ -Fe<sub>2</sub>O<sub>3</sub> nanoparticles in copolymer matrix  
at room temperature

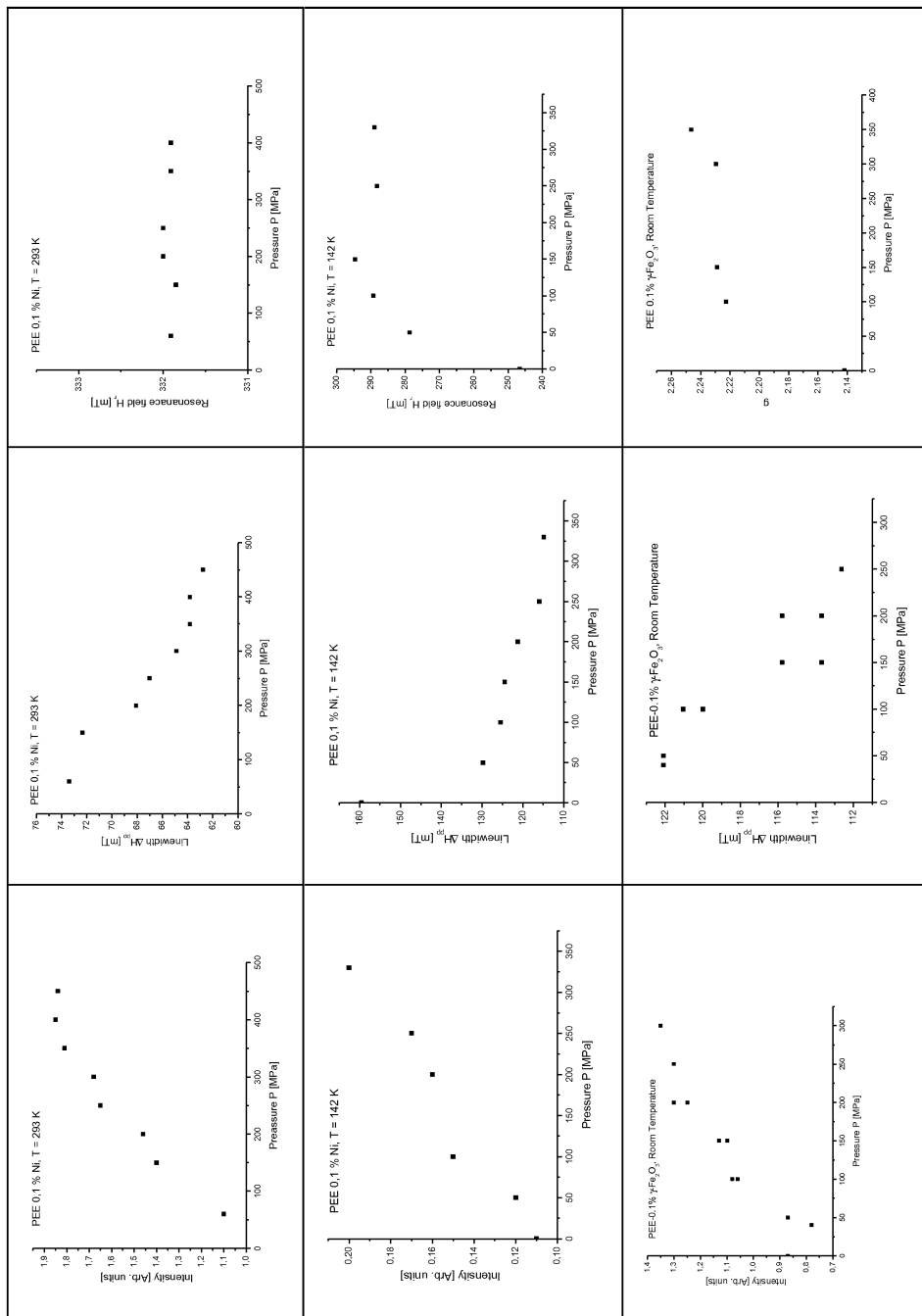
N. Gouskos<sup>1,2</sup>, A. Krupska<sup>3</sup>, J. Typek<sup>2</sup>

<sup>1</sup>*Department of Solid State Physics, Faculty of Physics, University of Athens  
Panepistimiopolis, 15 784 Zografou, Athens, Greece*

<sup>2</sup>*Institute of Physics, West Pomeranian University of Technology  
Al. Piastów 48, 70-311 Szczecin, Poland*

<sup>3</sup>*Institute of Molecular Physics, Polish Academy of Science  
M. Smoluchowskiego 17, 60-179 Poznan, Poland*

The pressure dependence of the ferromagnetic resonance (FMR) spectra of two samples consisting of 0.1%  $\gamma$ -Fe<sub>2</sub>O<sub>3</sub> and Ni nanoparticles embedded in a nonmagnetic polymer matrix was investigated at room temperature (RT) and one of them was studied at 142 K. Significant variations of the FMR parameters were observed as a function of the applied external pressure for both samples. It was demonstrated that the pressure dependence of the FMR parameters as a linewidth and integrated intensity was similar but the resonance field for the sample with nickel did not change at RT. The results are presented on the next page.



# Photoacoustic response of red fruit *Pyracantha Coccinea*

N. Guskos<sup>1,2</sup>, J. Majszczyk<sup>2</sup>, J. Typek<sup>2</sup>, A. Guskos<sup>2</sup>, J. Rybicki<sup>3</sup>

<sup>1</sup>*Department of Solid State Physics, Faculty of Physics, University of Athens  
Panepistimiopolis, 15 784 Zografou, Athens, Greece*

<sup>2</sup>*Institute of Physics, West Pomeranian University of Technology  
Al. Piastów 17, 70-310 Szczecin, Poland*

<sup>3</sup>*Department of Solid State Physics, Faculty of Applied Physics and Mathematics  
Gdansk University of Technology  
Narutowicza 11/12, 80-233 Gdansk, Poland*

A sample of red fruit *Pyracantha Coccinea* was prepared in a thick film form to study the photoacoustic (PA) response. One absorption band in the visible range, peaking at about 546 nm, and another at about 665 nm were registered in the visible range of EM radiation while absorption bands attributed to the  $\pi \rightarrow \pi^*$ ,  $\pi \rightarrow n$  charge transitions were detected in the ultraviolet range. The absorption band at 665 nm could be connected with the photosynthesis processes. This absorption band in the PA spectrum was very similar to a spectrum of *Ficus Benjamina* leaves obtained earlier [1]. The absorption band near 546 nm was similar to the one obtained for spermidine, being of importance in the information transfer to DNA [2]. The results obtained are significant, confirming experimentally that red fruit *Pyracantha Coccinea* absorb particularly intensely in that part of the solar radiation for which water is transparent.

## References

- [1] N. Guskos, G. Papadopoulos, J. Majszczyk, J. Typek, M. Wabia, D. G. Paschalidis, V. Likodimos, I. A. Tossidis, K. Aidinis, *Acta Phys. Pol. A* 103, 301 (2003).
- [2] N. Guskos, J. Majszczyk, J. Typek, J. Rybicki, submitted for publication

---

Magnetic properties of composites of  $\gamma$ -Fe<sub>2</sub>O<sub>3</sub> nanoparticles covered by Me<sub>3</sub>[Fe(CN)<sub>6</sub>]<sub>2</sub>·H<sub>2</sub>O (Me(II) = Co(II) and Ni(II))

N. Gouskos<sup>1,2</sup>, D. Petridis<sup>3</sup>, S. Glenis<sup>1</sup>, A. Guskos<sup>2</sup>, P. Berczyński<sup>2</sup>

<sup>1</sup>*Department of Solid State Physics, Faculty of Physics, University of Athens  
Panepistimiopolis, 15 784 Zografou, Athens, Greece*

<sup>2</sup>*Institute of Physics, West Pomeranian University of Technology  
Al. Piastów 48, 70-311 Szczecin, Poland*

<sup>3</sup>*NCSR "Demokritos", Aghia Paraskevi  
Attikis, Athens, Greece*

The magnetic properties of two composites of  $\gamma$ -Fe<sub>2</sub>O<sub>3</sub> nanoparticles covered by molecular magnets of Me<sub>3</sub>[Fe(CN)<sub>6</sub>]<sub>2</sub>·H<sub>2</sub>O (Me(II) = Co(II) and Ni(II)) were studied. The temperature dependence of ZFC and FC modes was obtained for a different applied magnetic fields. Additional magnetic field dependence of magnetization was recorded at different temperatures (Fig. 1 on the next page). For a sample with cobalt, at the applied magnetic field of 50 Oe, the blocking was unobserved up to the temperature of 350 K, while at 500 Oe the blocking was observed at 300 K. For a system with nickel the blocking temperature was much lower at low values of the applied magnetic field. At low temperatures, in both cases hysteresis loops were obtained but only for a system of cobalt up to 320 K.

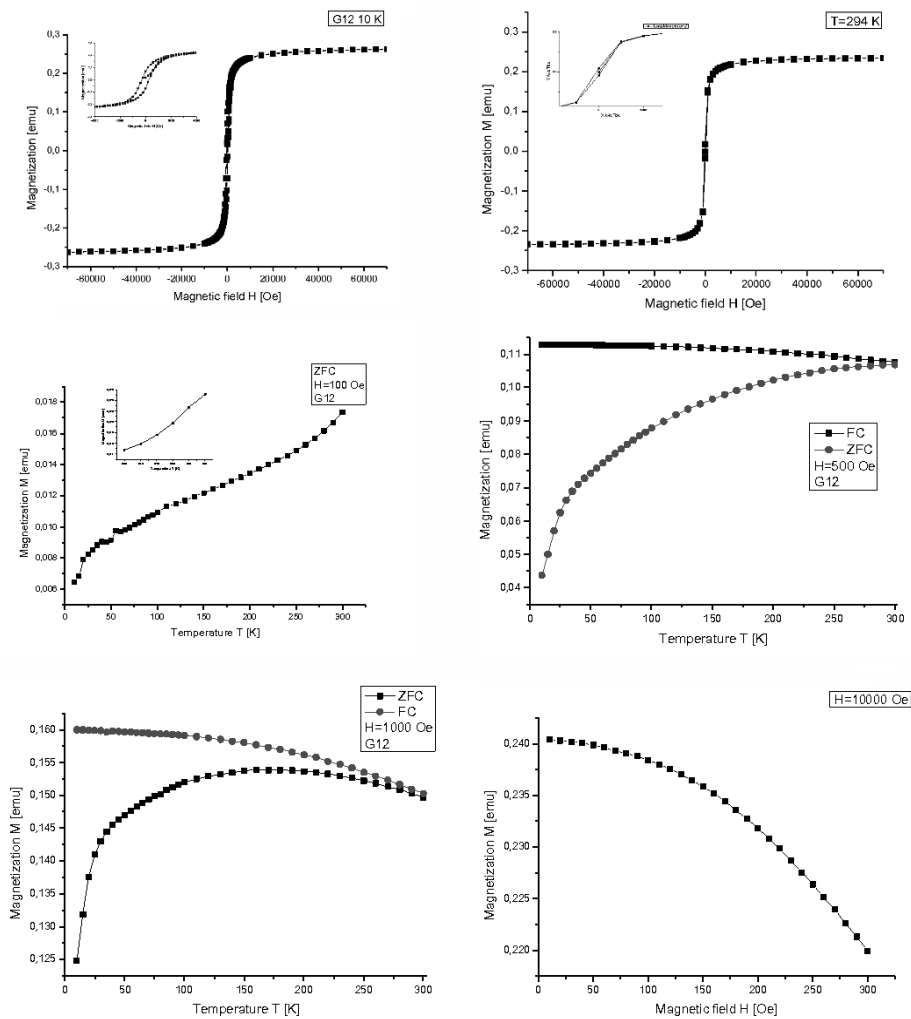


Figure 1: Magnetic measurements of sample  $\text{Co}_3[\text{Fe}(\text{CN})_6]_2 \cdot \text{H}_2\text{O}$

---

Temperature dependence study of EPR/FMR  
spectra of nanocrystalline  $n\text{MnO}/(1-n)\text{ZnO}$   
( $n = 0.20, 0.30, 0.40$ )

N. Gouskos<sup>1,2</sup>, G. Żołnierkiewicz<sup>2</sup>, J. Typek<sup>2</sup>,  
D. Sibera<sup>3</sup>, U. Narkiewicz<sup>3</sup>

<sup>1</sup>*Department of Solid State Physics, Faculty of Physics, University of Athens  
Panepistimiopolis, 15 784 Zografou, Athens, Greece*

<sup>2</sup>*Institute of Physics, Faculty of Mechanical Engineering and Mechatronics  
West Pomeranian University of Technology  
Al. Piastów 48, 70-311 Szczecin, Poland*

<sup>3</sup>*Institute of Chemical and Environmental Engineering  
West Pomeranian University of Technology  
Al. Piastów 17, 70-310 Szczecin, Poland*

The magnetic properties of nanocrystalline  $n\text{MnO}/(1-n)\text{ZnO}$  ( $n = 0.20, 0.30$  and  $0.40$ ) were studied. The samples were characterized by XRD that revealed the presence of ZnO and  $\text{ZnMnO}_3$  phases. An average size of magnetic  $\text{ZnMnO}_3$  nanocrystallites was found to be 9 nm. The EPR/FMR spectra were studied in the 4–300 K range and attributed to three different magnetic centers: two centers were attributed to the localized spins (defects of manganese ions and clusters) and one to the magnetic nanoparticles. The study of the resonance field temperature dependence, linewidth and integrated intensity showed very interesting behavior. The intensity of the magnetic  $\text{ZnMnO}_3$  FMR spectrum increased strongly with an increase in the composition index  $n$ . The relaxation processes were found to be different for magnetic localized centers and magnetic clusters.

## Modelling of auxetic biomedical devices

J. N. Grima<sup>1,2</sup>, A. Casha<sup>1,3</sup>, R. Gatt<sup>1</sup>, K. Dudek<sup>1</sup>,  
W. Wolak<sup>1</sup>, D. Attard<sup>1</sup>

<sup>1</sup>*Metamaterials Unit, Faculty of Science, University of Malta  
Msida MSD 2080, Malta*

<sup>2</sup>*Department of Chemistry, Faculty of Science, University of Malta  
Msida MSD 2080, Malta*

<sup>3</sup>*Faculty of Medicine and Surgery, University of Malta  
Msida MSD 2080, Malta*

This paper deals with the applications of auxetic materials in the field of medical devices and looks at the application of auxetics within patients or applied to patients and to devices that are used in the medical field.

In particular the use of auxetic and related systems in the design of stents is discussed.

The exponential increase in patents granted worldwide for applications of auxetic materials indicates that future developments in this field will be exciting especially in biomedical applications.

### **Acknowledgements**

The support of the University of Malta, the Malta Council for Science and Technology and the Commerce Division (Malta) is gratefully acknowledged.

---

# Melting phenomena in platinum nanoclusters

P. Kajak<sup>1</sup>, J. Rybicki<sup>1,2,3</sup>

<sup>1</sup>*Department of Solid State Physics, Gdansk University of Technology  
Narutowicza 11/12, 80-233 Gdansk, Poland*

<sup>2</sup>*TASK Computer Center, Gdansk University of Technology  
Narutowicza 11/12, 80-233 Gdansk, Poland*

<sup>3</sup>*Institute of Mechatronics, Nanotechnology and Vacuum Techniques  
Koszalin University of Technology  
Raclawicka 5-17, 75-620 Koszalin, Poland*

Platinum clusters are of major importance for the future development of nanodevices. Due to its physical and chemical properties platinum is widely used as a catalyst as well as alloying agent for various metal products.

In this work the results of molecular dynamics studies on melting phenomena in platinum nanoclusters are presented. Spherical clusters of diameters ranging from 2 nm to 8 nm heated from 300 K to 2000 K were investigated. The transition temperatures, the radial distributions of the diffusion coefficient and the freezing/melting hysteresis were analyzed.

Our preliminary results show that cluster melting can be divided into two stages. In the first liquid outside skin is formed and maintained until the second stage when a rapid phase transition develops in the entire cluster.

## **Acknowledgements**

This work has been sponsored by the Ministry of Science and Higher Education, under research grant number N N519 577838. The calculations were performed at the TASK Computer Center, Gdansk, Poland.

# The pretransitional fluctuations in liquid crystalline materials studied by nonlinear dielectric spectroscopy

P. Kędziora

*Institute of Molecular Physics, Polish Academy of Sciences  
Smoluchowskiego 17, 60-179 Poznań, Poland*

The nonlinear dielectric spectroscopy (NDS) is one of useful methods to study the kinetics of intermolecular aggregations processes, conformational changes and strong intermolecular orientational correlations, such as those existing in liquid crystalline materials.

The studies of the pretransitional behavior in the isotropic phase of mesogenic substance in the vicinity of the nematic and smectic phase transitions have shown universality of the critical-like behavior of the dielectric properties for different mesogenic systems. There are spectroscopic evidences for the existence of an equilibrium between the pseudo-nematic domains and the freely moving mesogenic molecules [1,2].

Some molecular fluctuations in the chiral nematic phase ( $N^*$ ), in the vicinity of the phase transition to the blue phase (BP), were also found and are limited to a very narrow interval of the temperature (2 K) between BP and  $N^*$ . The fluctuations manifest themselves as domains with supercooled blue phase structure. An appearance of the blue phase seems to exclude the existence of the pretransitional fluctuations in the isotropic phase [3].

The NDS allows one to study the orientational relaxation modes for a molecule in an isotropic fluid and in liquid crystalline phases. The studies of cholesteryl oleyl carbonate have shown that in the isotropic phase the molecule exhibits only one relaxation mode relevant to rotations of the longitudinal permanent dipole moment around the short axis. In the mesogenic phases the reorientation of dipole moment can be described by two or three modes.

## Acknowledgements

This work was supported by the Fonds voor Wetenschappelijk Onderzoek – Vlaanderen, Belgium, in the framework of the agreement for scientific cooperation with the Polish Academy of Sciences.

## References

- [1] P. Kędziora, J. Jadżyn, L. Hellemans, *Phys. Rev. E*, **66**, 031702 (2002)
- [2] P. Kędziora, *Liq. Crystals*, **39**, 425 (2012)
- [3] P. Kędziora, K. W. Wojciechowski, *J.Phys. Chem. B*, **113**, 9123 (2009)

---

## Structural investigations of nitrated VN-SiO<sub>2</sub> sol-gel derived films

B. Kościelska, A. Witkowska, L. Wicikowski

*Department of Solid State Physics, Gdansk University of Technology  
Narutowicza 11/12, 80-233 Gdansk, Poland*

In recent years much attention has been paid to nitride and oxynitride thin films, in particular to vanadium nitride films. Vanadium nitride is suitable for many uses due to its extreme hardness, wear resistance, excellent oxidative stability, corrosion resistance and high-temperature stability. From the technological point of view, VN is an important industrial catalyst. Moreover, with a superconducting transition temperature of 9 K, VN may be used in several superconducting microelectronics applications. It should be also underlined that a small addition of silicon oxide to the VN film improves its superconducting properties [1,2]. However, the origin of this behavior is not clear.

In the present work vanadium oxide films were prepared by thermal nitridation (with ammonia) of sol-gel derived V<sub>2</sub>O<sub>3</sub> films. In films prepared in such a way, homogeneous distribution of nitrogen is very important because the presence of a zone with a nitrogen deficiency or excess can change the properties of the layer. For future applications, it is crucial to know whether and how the VN/SiO<sub>2</sub> molar ratio and the film thickness influence their properties. Structural investigations of VN/SiO<sub>2</sub> films were performed with a few methods. Two near-edge (XANES) and extended (EXAFS) X-ray absorption fine structure spectra at V K-edge (5465 eV) were collected. The XAFS experiment was performed at XAFS 11.1 beamline station at ELETTRA. Scanning electron microscopy images and nanohardness measurements of the films were taken.

### References

- [1] Kościelska B., Winiarski A., Jurga W., 2010 *J. Non-Cryst. Solids* **356** 1998
- [2] Kościelska B., Yuzepovich O. I., Bengus S. V., Winiarski A., Sadowski W., Lapinski M., 2012 *Acta. Phys. Pol. A* **121** 332

## Optical properties of ceramic nanoparticles

S. P. Kruchinin, A. A. Zolotovskiy

*Bogolyubov Institute for Theoretical Physics  
NASU, Kiev 03143, Ukraine*

*Institute of Semiconductor Physics of the National Academy of Sciences of Ukraine  
45, Prosp. Nauky, Kyiv 03028, Ukraine*

The mechanism of formation of electron pairs in nanoparticles of ceramics was studied. The influence of second-order phase transitions in nanoparticles on the optical and magnetic properties were analyzed within the multielectron hybrid method.

---

# Crystallization kinetics of multiphase reactive blends in the presence of nanostructured additives

M. Kwiatkowska, K. Kwiatkowski

*Institute of Materials Science and Engineering  
West Pomeranian University of Technology Szczecin  
Al. Piastów 48, 70-311 Szczecin, Poland*

Due to their chemical structure, multiphase reactive blends based on poly(ethylene terephthalate) (PET) are classified as block copolymers with properties typical for thermoplastic elastomers (TPE). They exhibit a unique combination of strength, elasticity, and processability due to their microstructure. In general, they are composed of two different segments, commonly referred to as flexible and rigid segments. The flexible segments are derived from oligomers having a low glass transition temperature ( $T_g$ ), imparting flexibility to the polymer, whilst rigid segments with relatively high  $T_g$  should be able to crystallize. Crystallization of rigid segments is a key factor in polymer blends, as it forces the phase separation with formation of nanodomains serving as thermally reversible physical cross-links. The presence of crystalline areas accounts for the strength and dimensional stability of the polymer. From a practical viewpoint, a higher ability and rate of crystallization of rigid segments leads to a decrease in the processing time and energy consumption, which is positive also in economic terms.

Although PET is a very suitable candidate as an ester rigid segment for preparation of poly(ether-ester) copolymers (PEE), due to its lower tendency to crystallize and a lower rate of crystallization than the poly(butylene terephthalate) (PBT), it has not found application in the commercially available PEE copolymers. The way to support the crystallization process is to introduce crystallization promoters into the copolymer, facilitating the nucleation and crystallite growth. In this study the effect of different kinds of additives on the PET-PTMO crystallization process was analyzed. In addition to the typically used nucleation agents such as talc and  $\text{CaCO}_3$  it was also nanostructured additives such as: carbon nanotubes and nanofibres, silicon carbide (SiC) and iron carbide ( $\text{Fe}_2\text{C}_3$ ) that were incorporated into the copolymer during reactive blending. Based on the DSC measurements, the nucleation rate, the thermal effects,  $T_g$  and  $T_c$  values as well as the crystallinity degrees were determined in order to indicate the most suitable PET crystallization promoters.

## **Acknowledgements**

The research was financed by the Polish Ministry of Science and Higher Education from the resources for the years of 2009–2011 as a research project.

# Ferromagnetic resonance study of carbon coated nickel and cobalt nanoparticles

I. E. Lipiński<sup>1</sup>, M. Soboń<sup>2</sup>

<sup>1</sup>*Institute of Physics, Faculty of Mechanical Engineering and Mechatronics  
West Pomeranian University of Technology  
Al. Piastów 17, 70-311 Szczecin, Poland*

<sup>2</sup>*The Faculty of Management and Economic of Services, University of Szczecin  
Cukrowa 8, 71-004 Szczecin, Poland*

Two types of samples of agglomerated cobalt and nickel magnetic nanoparticles coated with carbon dispersed in a paraffin matrix were studied. Ferromagnetic resonance (FMR) spectra were recorded at room temperature.

Both samples showed a very intense and broad asymmetric FMR line arising from the cobalt and nickel nanoparticles but the samples with nickel, in spite of a similar structure compared to cobalt, presented quite different spectra. In order to obtain the value of the magnetic resonance fields and line widths, the FMR spectra were fitted as a sum of functions representing both the absorption and dispersion in these materials. We try to explain the differences in the FMR spectra and magnetic interactions in terms of the preparation procedure of the samples.

---

# Structural investigations of lithium titanate spinel oxide nanopowder prepared by low temperature method

M. Łapiński, A. Bojarska, B. Kościelska, W. Sadowski

*Department of Solid State Physics, Gdansk University of Technology  
Narutowicza 11/12, 80-233 Gdansk, Poland*

Lithium titanate spinel oxide ( $\text{LiTi}_2\text{O}_4$ ) has been the subject of vast research due to its good electrical properties at room temperature and superconductive behavior below 13 K. Owing to these features, lithium titanate is a very popular compound, especially as an electrode material for rechargeable batteries [1,2,3].

One of the most widespread methods used for preparation of  $\text{LiTi}_2\text{O}_4$  is the solid state reaction. Typically, samples are synthesized using titanium oxides and lithium carbonate as precursors. Then, they are calcinated at the temperature in a range from  $750^\circ\text{C}$  to  $800^\circ\text{C}$  [4,5].

In this work, a new low temperature preparation method is presented. Lithium titanate powder samples were prepared using the sol-gel method. Lithium acetate, butoxytitanium and ethanol were used as the reagents. Formation of nanocrystalline phase was conducted during annealing for 20 hours at temperature range spanning from  $500^\circ\text{C}$  to  $600^\circ\text{C}$  in the argon atmosphere. The structure of the prepared material was investigated by the X-Ray Diffraction method, while the sample's morphology was studied by Scanning Electron Microscope. A correlation between the temperature of calcination and the structure of manufactured films was shown.

## References

- [1] Geng H. X., Dong A. F., Che G. C., Huang W. W., Jia S. L., Zhao Z. X. 2005 *Physica C* **432** 53
- [2] Kanno T., Awaka J., Kariya F., Bisu S., Nagata S. 2006 *Physica B* **381** 30
- [3] Łapinski M., Kościelska B., Sadowski W. 2012 *J. Alloy. Compd.* <http://dx.doi.org/10.1016/j.jallcom.2012.04.100>
- [4] Moshopoulou E. G. 1999 *J. Am. Ceram. Soc* **82** 3317
- [5] Feng C. Q., Li L., Guo Z. P., Shi D. Q., Zeng R., Zhu X. J. 2009 *J. Alloy. Compd* **478** 767

# Partially auxetic behavior in fcc crystals of soft polydisperse dimers

J. W. Narojczyk, M. Kowalik, K. W. Wojciechowski

*Institute of Molecular Physics, Polish Academy of Sciences  
M. Smoluchowskiego 17, 60-179 Poznań, Poland*

Materials exhibiting anomalous (negative) Poisson's ratio called auxetics have been the subject of increasing interest recently [1]. This work is aimed at extending the knowledge about the effect of atomic size polydispersity on the macroscopic elastic properties of a three-dimensional system of dimers forming the degenerate crystalline phase (DC) [2]. The model, with purely repulsive nearest neighbor interactions, was studied by computer simulations at zero temperature by a method described earlier [3].

It is known that rising the particle size polydispersity usually results in an increase in Poisson's ratio [4–8] in both isotropic and anisotropic systems. However, it has been recently found that in the case of some three-dimensional cubic systems, it is possible for Poisson's ratio to *decrease* [9,10] down to negative values in some crystalline directions along with an increase in the atomic size polydispersity. In the case of soft polydisperse spheres [9] a significant decrease in Poisson's ratio was observed for soft interactions, whereas in the case of dc dimers, Poisson's ratio decreased when the interaction potential hardened [10] what may be of interest in practical applications. The latter study concerned a model where the sizes of the atoms forming a dimer were independent of each other and the distance between their centers was fixed to the average diameter of all the atoms in the system [10]. However, such a constraint may be inconvenient in practice. Thus, two other variants of the model are proposed in this work whereby the aforementioned shortcoming may be alleviated. In the first variant, the sizes of the atoms forming each dimer are no longer independent – their sum is always equal to the dimer bond length. In the second variant, the bond length polydispersity is introduced, whereby the dimer's atoms can be kept adjacent while retaining freedom in the choice of their size.

It has been found that both the new variants of the dimer model show similar behavior as the previously studied model what may be of importance while designing new materials with negative Poisson's ratio.

## Acknowledgements

This work was partially supported by grant NN202261438 of the Polish Ministry of Science and Education. Some simulations were performed at the Poznań Supercomputing and Networking Center (PCSS).

## References

- [1] R. Gatt, J. N. Grima, J. W. Narojczyk, and K. W. Wojciechowski. Auxetic materials and related systems. *Physica Status Solidi (b)*, 249: 1313–1314, 2012; see also references therein.

- 
- [2] K. W. Wojciechowski. Degenerate crystalline phase in a two-dimensional system of hard dimers. *Modern Physics Letters b*, 5: 1843–1851, 1991.
  - [3] J. W. Narojczyk and K. W. Wojciechowski. Elastic properties of two-dimensional soft polydisperse trimers at zero temperature. *Physica Status Solidi (b)*, 244: 943–954, 2007.
  - [4] K. W. Wojciechowski and J. Narojczyk. Influence of disorder on the Poisson’s ratio of static solids in two dimensions. *Reviews on Advanced Materials Science*, 12: 120–126, 2006.
  - [5] J. W. Narojczyk and K. W. Wojciechowski. Computer simulation of the Poisson’s ratio of soft polydisperse discs at zero temperature. *Materials Science (Poland)*, 24: 921–927, 2006.
  - [6] J. W. Narojczyk and K. W. Wojciechowski. Elastic properties of two-dimensional soft discs of various diameters at zero temperature. *Journal of Non-Crystalline Solids*, 352: 4292–4298, 2006.
  - [7] J. W. Narojczyk and K. W. Wojciechowski. Elasticity of periodic and aperiodic structures of polydisperse dimers in two dimensions at zero temperature. *Physica Status Solidi (b)*, 245: 2463–2468, 2008.
  - [8] J. W. Narojczyk, A. Alderson, A. R. Imre, F. Scarpa, and K. W. Wojciechowski. Negative Poisson’s ratio behavior in the planar model of asymmetric trimers at zero temperature. *Journal of Non-Crystalline Solids*, 354: 4242–4248, 2008.
  - [9] J. W. Narojczyk and K. W. Wojciechowski. Elastic properties of the fcc crystals of soft spheres with size dispersion at zero temperature. *Physica Status Solidi (b)*, 245: 606–613, 2008.
  - [10] J. W. Narojczyk and K. W. Wojciechowski. Elastic properties of degenerate f.c.c. crystal of polydisperse soft dimers at zero temperature. *Journal of Non-crystalline Solids*, 356: 2026–2032, 2010.

## Structure and spectroscopic properties of undoped borate glasses

B. V. Padlyak<sup>1,2</sup>, A. Drzewiecki<sup>1</sup>, S. I. Mudry<sup>3</sup>, Yu. O. Kulyk<sup>3</sup>

<sup>1</sup>*Division of Spectroscopy of Functional Materials, Institute of Physics  
University of Zielona Góra  
Szafrana 4a, 65-516 Zielona Góra, Poland*

<sup>2</sup>*Sector of Spectroscopy, Institute of Physical Optics  
Dragomanova 23, 79-005 Lviv, Ukraine*

<sup>3</sup>*Department of Physics, Ivan Franko National University of Lviv  
Kyryla i Mefodiya 6, 79-005 Lviv, Ukraine*

A series of borate glasses ( $\text{Li}_2\text{B}_4\text{O}_7$ ,  $\text{LiKB}_4\text{O}_7$ ,  $\text{LiB}_3\text{O}_5$ ,  $\text{CaB}_4\text{O}_7$ ,  $\text{SrB}_4\text{O}_7$ , and  $\text{LiCaBO}_3$ ) of high optical quality and chemical purity were obtained from corresponding polycrystalline compounds using the standard glass technology. The X-ray diffraction intensity profiles of the investigated glasses were typical of glassy compounds. The most typical intensity profile, consisting of almost symmetrical peaks, was observed in the case of  $\text{Li}_2\text{B}_4\text{O}_7$  and  $\text{LiB}_3\text{O}_5$  glasses. Substitution and partial substitution of Li atoms by Sr and Ca atoms was accompanied by significant changes in the intensity profiles of the investigated glasses. Pair correlation functions and structural parameters (most probable interatomic distances and coordination number to oxygen) of the investigated glasses were evaluated and analyzed. Structural peculiarities of the investigated borate glasses are discussed in comparison with the structural data available for their crystalline analogs.

The electron paramagnetic resonance (EPR), optical absorption and photoluminescence spectra of the undoped glasses with  $\text{Li}_2\text{B}_4\text{O}_7$ ,  $\text{LiKB}_4\text{O}_7$ ,  $\text{CaB}_4\text{O}_7$ , and  $\text{LiCaBO}_3$  compositions were investigated and analyzed. In all undoped glasses the EPR signal, characteristic of the glassy state, ( $g_{eff} \cong 4.3$ ) of the  $\text{Fe}^{3+}$  ( $3d^5$ ,  ${}^6S_{5/2}$ ) non-controlled impurity was observed. The obtained glasses are characterized by high transparency in the 350–1300 nm spectral range. The optical absorption edge for all the obtained glasses was analyzed using the Urbach rule. The optical band gap and Urbach energy for the investigated glasses were determined. All undoped borate glasses under UV excitation at room temperature revealed broad (350–550 nm) complex emission bands peaked around 450 nm which were assigned to the intrinsic luminescence. The recombination mechanism of the intrinsic luminescence in borate glasses was considered and discussed.

### Acknowledgements

This work was supported by the Ministry of Education, Science, Youth and Sport of Ukraine (Project No. 0111U001627) and the University of Zielona Góra (Poland).

# Optical and EPR spectroscopy of $\text{Li}_2\text{B}_4\text{O}_7:\text{Er}$ glasses

B. V. Padlyak<sup>1,2</sup>, W. Ryba-Romanowski<sup>3</sup>, R. Lisiecki<sup>3</sup>,  
N. Gouskos<sup>4,5</sup>, G. Żołnierkiewicz<sup>5</sup>

<sup>1</sup>*Division of Spectroscopy of Functional Materials  
Institute of Physics, University of Zielona Góra  
Szafrana 4a, 65-516 Zielona Góra, Poland*

<sup>2</sup>*Institute of Physical Optics, Sector of Spectroscopy  
Dragomanov 23, 79-005 Lviv, Ukraine*

<sup>3</sup>*Institute of Low Temperatures and Structure Research of the Polish Academy of Sciences  
Okólna 2, 50-422 Wrocław, Poland*

<sup>4</sup>*Solid State Physics Section, Department of Physics, University of Athens  
Panepistimiopolis, 15 784 Zografou, Athens, Greece*

<sup>5</sup>*Institute of Physics, West Pomeranian University of Technology  
Al. Piastów 17, 70-310 Szczecin, Poland*

Lithium tetraborate glasses doped with erbium ( $\text{Li}_2\text{B}_4\text{O}_7:\text{Er}$ ) were investigated by electron paramagnetic resonance (EPR) at liquid helium temperatures and optical spectroscopy at room temperature. ( $\text{Li}_2\text{B}_4\text{O}_7:\text{Er}$ ) glasses of high optical quality were obtained from corresponding polycrystalline compounds by standard technology of borate glasses presented in [1]. The erbium (Er) impurity was added to the raw materials as the  $\text{Er}_2\text{O}_3$  compound in the amounts of 0.5 and 1.0 mol.%.

The EPR and optical spectroscopy methods showed that the Er impurity was incorporated into the glass network as  $\text{Er}^{3+}$  ions (4f<sup>11</sup> electron configuration,  $^4\text{I}_{15/2}$  free ion ground state), exclusively. All the observed  $f-f$  transitions of the  $\text{Er}^{3+}$  ions in the optical spectra of the  $\text{Li}_2\text{B}_4\text{O}_7:\text{Er}$  glasses were identified and EPR signals were interpreted.

The ground state optical absorption, luminescence excitation, and emission spectra as well as luminescence kinetics for the main transitions of the  $\text{Er}^{3+}$  centers in the  $\text{Li}_2\text{B}_4\text{O}_7:\text{Er}$  glasses were investigated and analyzed. On the basis of the standard Judd-Ofelt theory the oscillator strengths ( $P_{\text{theor}}$ ) for all the observed absorption transitions and phenomenological intensity parameters ( $\Omega_2$ ,  $\Omega_4$ , and  $\Omega_6$ ) of the  $\text{Er}^{3+}$  centers in  $\text{Li}_2\text{B}_4\text{O}_7:\text{Er}$  glasses were calculated and compared with the corresponding parameters, obtained for other borate glasses and crystals. Spectroscopic parameters of relevance for laser applications, including radiative decay rates (emission probabilities of transitions),  $W_r$ , branching ratios,  $\beta$ , and radiative lifetimes,  $\tau_{\text{rad}}$ , were calculated for all the main electric dipole transitions of the  $\text{Er}^{3+}$  centers in the  $\text{Li}_2\text{B}_4\text{O}_7:\text{Er}$  glasses.

The luminescence kinetics for the infrared emission band ( $^4\text{I}_{13/2} \rightarrow ^4\text{I}_{15/2}$  transition,  $\lambda_{\text{max}} \cong 1531$  nm) of the  $\text{Er}^{3+}$  centers was satisfactorily described by the single exponential decay, whereas the luminescence kinetics for the green emission band

( ${}^4S_{3/2} \rightarrow {}^4I_{15/2}$  transition,  $\lambda_{\max} \cong 563$  nm) of the  $\text{Er}^{3+}$  centers was described by non-exponential decay with average lifetime values. The Obtained experimental lifetimes were compared with those calculated and the quantum efficiency ( $\eta$ ) for green and infrared emission transitions was estimated and compared with the corresponding quantum efficiencies of the  $\text{Er}^{3+}$  laser glasses and crystals. The prospects of applications of the  $\text{Li}_2\text{B}_4\text{O}_7:\text{Er}$  glasses for solid-state lasers operating in green ( ${}^4S_{3/2} \rightarrow {}^4I_{15/2}$  channel) and infrared eye-safe ( ${}^4I_{13/2} \rightarrow {}^4I_{15/2}$  channel) spectral regions were considered.

The incorporation peculiarities and local structure of the  $\text{Er}^{3+}$  luminescence centers in the  $\text{Li}_2\text{B}_4\text{O}_7:\text{Er}$  glass network were considered and discussed based on the referenced structural data for glass [1] and crystal [2] with the  $\text{Li}_2\text{B}_4\text{O}_7$  composition and obtained spectroscopic results.

### Acknowledgements

This work was supported by the Ministry of Education, Science, Youth and Sport of Ukraine (Project No. 0111U001627) and the University of Zielona Góra (Poland).

### References

- [1] B. V. Padlyak, S. I. Mudry, Yu. O. Kulyk, O. O. Smyrnov, A. Drzewicki, V. T. Adamiv, Ya. V. Burak, I. M. Teslyuk 2010 “V International Conference on Physics of Disordered Systems (PDS’2010)” Gdansk-Sobieszewo (Poland) Abstract Book, 176-177.
- [2] J. Krogh-Moe 1968 Acta Cryst. B **24** 179.

# Negative mechanical compliance of constrained auxetic materials

A. A. Poźniak<sup>1</sup>, K. W. Wojciechowski<sup>2</sup>

<sup>1</sup>*Institute of Physics, Poznań University of Technology  
Nieszawska 13A, 60-965 Poznań, Poland*

<sup>2</sup>*Institute of Molecular Physics, Polish Academy of Sciences  
M. Smoluchowskiego 17/19, 60-179 Poznań, Poland*

Materials characterized by negative Poisson's ratio (PR), often called auxetics, expand transversely when stretched axially. Auxetics constrained in a certain way reveal another counterintuitive effect – negative mechanical compliance [1,2].

The model considered here consists of a square continuum (pure 2D elasticity) with fixed horizontal boundaries. The remaining boundaries are under pressure pushing the edges inward. It turned out that this system behaved like one with (locally) negative mechanical compliance [2]. This conclusion was based on the observation of the deformed shape of non-constrained edges which locally deformed against the acting force. Qualitatively equivalent behaviour was observed when the external pressure was replaced by a uniform gravitational field acting on the body mass of the sample.

Critical PR was determined depending on the mesh density being PR for which a single node of the mesh had a component opposite to the acting force. Using proper fitting functions it was shown that critical PR tended to zero as the mesh density increased to infinity, which represented the exact solution.

Another interesting observation concerned the shape of the pushed edges. Namely, it was noticed that close to PR of  $-1$  those edges revealed more local maxima and minima, in other words they were more and more corrugated when PR tended to  $-1$ .

## Acknowledgements

This work was partially supported by grant NN202261438 of the Polish Ministry of Science and Education. Some calculations were performed at the Poznań Supercomputing and Networking Center (PCSS).

## References

- [1] T. Strek, B. Maruszewski, J. W. Narojczyk; K. W. Wojciechowski, *J. Non-Cryst. Solids* **354**, 4475–4480 (2008).
- [2] A. A. Poźniak; H. Kaminski, P. Kedziora, B. M. Maruszewski, T. Strek, K. W. Wojciechowski, *Rev. Adv. Mater. Sci.* **23**, 169–174 (2010).

# Impact of carbon nanotube on homocysteine clusters – MD simulation

P. Raczyński, M. Pabiszczak, Z. Gburski

*Institute of Physics, University of Silesia  
Uniwersytecka 4, 40-007 Katowice, Poland*

Excessive amounts of homocysteine in the human body have been recently considered as a factor which increases the risk of developing diseases in the cardiovascular system. Elevated levels of homocysteine have been linked to increased fractures in humans. The pure clusters composed of a finite number of homocysteine molecules were studied by the MD technique. Moreover, the impact of a capped carbon nanotube on homocysteine clusters was examined. The mean square displacement, the diffusion coefficient, the radial distribution function and the Lindeman index of homocysteine were calculated for several temperatures, including the physiological temperature  $T = 310$  K. We interpreted the behaviour of homocysteine molecules in pure clusters and in systems with a carbon nanotube by a qualitative interpretation of the physical observables and snapshots of instantaneous configurations. The anticipated applications of carbon nanotubes include the use of these materials for the design and development of biological sensors, the homocysteine nanosensor (carbon nanotube based) in this case.

# Poisson's ratio of polydisperse hard disks and spheres

K. V. Tretiakov, K. W. Wojciechowski

*Institute of Molecular Physics Polish Academy of Sciences  
M. Smoluchowskiego 17/19, 60-179 Poznań, Poland*

Polydisperse hard spheres are considered in three and two dimensions; the latter are further referred to as hard disks. These systems constitute basic models for real polydisperse systems such as colloidal suspensions [1] and granular materials [2].

The present research is focused on the effect of size polydispersity on the elastic properties of systems with special attention paid to Poisson's ratio. The simulations of hard disks [3] show that *any* amount of size polydispersity results in a discontinuous “jump” of Poisson's ratio in the close packing limit from the value  $\nu_{\delta=0} = 0.1308(22)$ , obtained for equidiameter hard disks [4], to  $\nu_{\delta>0} \approx 1$ , estimated for polydisperse disks (see Fig. 1a). Similar behavior is found for the fcc phase of polydisperse hard spheres [5] for which Poisson's ratio in main crystallographic directions “jumps: (i) in the [100] direction from the value  $\nu_{\delta=0} = 0.196(7)$  obtained for equidiameter hard spheres [6] to  $\nu_{\delta>0} \approx 0.5$  for polydisperse spheres (see Fig. 1b), and analogically (ii) in the [111] direction from  $\nu_{\delta=0} = 0.045(6)$  to  $\nu_{\delta>0} \approx 0.5$  (see Fig. 1c). It is also found that, in the range of the pressures studied, the extreme values of Poisson's ratio of polydisperse hard sphere systems correspond to the [110] direction. It is worth emphasizing that the system reveals *auxetic* behavior [7–9] (*i.e.* Poisson's ratio is negative) for all the polydispersities studied [5] for the pair of directions [110][1 $\bar{1}$ 0] at moderate pressures.

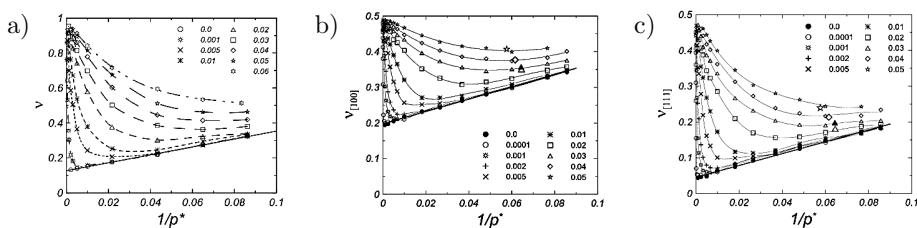


Figure 1: Inverse pressure dependence of Poisson's ratio of: (a) polydisperse hard disks [3], (b) polydisperse hard spheres in the [100] direction [5], and (c) the polydisperse hard spheres in the [111] direction [5]

## Acknowledgements

This work was supported by Grant NN202261438 of the Polish Ministry of Science and Education. Some calculations were performed at the Poznań Computing and Networking Center (PCSS).

## References

[1] R. P. Sear and D. Frenkel, Phys. Rev. E **55**, 1677 (1997).

- [2] I. S. Aranson and L. S. Tsimring, *Rev. Mod. Phys.* **78**, 641 (2006).
- [3] K. V. Tretyakov and K. W. Wojciechowski, *J. Chem. Phys.* **136**, 204506 (2012).
- [4] K. W. Wojciechowski, K. V. Tretyakov, A. C. Branka, and M. Kowalik, *J. Chem. Phys.* **119**, 939 (2003).
- [5] K. V. Tretyakov and K. W. Wojciechowski, to be published.
- [6] K. V. Tretyakov and K. W. Wojciechowski, *J. Chem. Phys.* **123**, 074509 (2003).
- [7] R. Lakes, *Science* **235**, 1038 (1987).
- [8] K. E. Evans, M. A. Nkansah, I. J. Hutchinson, and S. C. Rogers, *Nature* **353**, 124 (1991).
- [9] R. Gatt, J. N. Grima, J. W. Narojczyk, and K. W. Wojciechowski, *Phys. Stat. Solidi* **249**, 1313 (2012)

---

## Structure of small platinum clusters

S. Winczewski<sup>1</sup>, J. Rybicki<sup>1,2,3</sup>

<sup>1</sup>*Department of Solid State Physics, Gdansk University of Technology  
Narutowicza 11/12, 80-233 Gdansk, Poland*

<sup>2</sup>*TASK Computer Center, Gdansk University of Technology  
Narutowicza 11/12, 80-233 Gdansk, Poland*

<sup>3</sup>*Institute of Mechatronics, Nanotechnology and Vacuum Techniques  
Koszalin University of Technology  
Raclawicka 5-17, 75-620 Koszalin, Poland*

Platinum clusters are one of the most frequently investigated nano-sized systems. As a highly dispersed form of a chemically active element, they offer high intensity of a key catalytic process. Since they are considered most promising materials for fuel cell applications, it is obvious that one of the main and most challenging tasks for nanotechnologists is to control their properties.

This work presents the results of systematic studies on the structure of small platinum clusters consisting of 2–15 atoms. An extensive global search driven by a genetic algorithm and coupled with a semi-empirical description was performed. As a result, numerous stable configurations were located. The localized structures were then subjected to further local relaxation, employing DFT methods.

The obtained results show that up to 9 atom size planar and nearly planar arrangements are as stable as three dimensional ones. This trend turns into a tendency to prefer both distorted and disordered spatial structures beyond the 9 atom size. Based on the results, we conclude that the fcc-like structures are strongly preferred even for the region of early growth.

### **Acknowledgements**

This work has been sponsored by the Ministry of Science and Higher Education, under a research grant number N N519 577838. The calculations were performed at the TASK Computer Center, Gdansk, Poland.

# Platinum nano-particles embedded in acidic cesium or rubidium salt matrices: an XAS study

A. Witkowska<sup>1</sup>, S. Dsoke<sup>2</sup>, R. Marassi<sup>2</sup>, A. Di Cicco<sup>3,4</sup>

<sup>1</sup>*Department of Solid State Physics, Gdansk University of Technology  
Narutowicza 11/12, 80-233 Gdansk, Poland*

<sup>2</sup>*Chemistry Department, University of Camerino  
I-62032 Camerino (MC), Italy*

<sup>3</sup>*CNISM, School of Science and Technology, Physics Division, University of Camerino  
I-62032 Camerino (MC), Italy*

<sup>4</sup>*IMPMC-CNRS, Université P.et M. Curie  
Campus Jussieu, 4 place Jussieu, F-75005 Paris, France*

We present an X-ray absorption spectroscopy (XAS) study of a novel Pt-based catalyst operating at low temperature fuel cells (FCs). These fuel cells generally utilize solid polymer electrolytes and they are a promising class of compact devices representing a future alternative to fossil-fuel based engines. Until now one of the most challenging goals in the development of low temperature FCs has been to accelerate the too slow oxygen reduction reaction (ORR) and limit the requested amount of Pt in the catalyst [1,2]. A significant decrease in the Pt loading during the last two decades accompanied by tangible improvements of the power density has been achieved [3]. The result has been obtained mainly by diminishing the metal grain size to the nanometric scale and by improving the homogeneity of the nano-catalysts dispersion on the support. The innovation in the case of the considered catalyst resides in the use of a porous inorganic matrix of the composition  $X_{2.5}H_{0.5}YMo_{12}O_{40}$ ,  $X = Cs, Rb$  and  $Y = P, Si$  as a catalyst support [4,5]. Platinum ions were introduced to the mixture of Vulcan, Nafion and proper heteropolyacids salt using the electrochemical method to prepare the catalytic layer.

The pore size in the Keggin-type heteropolyacid salts can be controlled by the kind of cation used and the cation content. As most of the nanoparticles deposited on this kind of a matrix are embedded into the matrix pores, their size can be precisely controlled. The relation between the matrix composition and the size of the obtained nanoparticles was determined mainly by means of X-ray absorption spectroscopy [6] and the TEM image analysis. The details of the X-ray absorption fine structure (XAFS) data analysis are described in Refs [7,8,9].

## Acknowledgements

We gratefully acknowledge the support of the European Synchrotron Radiation Facility (Grenoble, France) in providing the synchrotron radiation facilities for the ch-2446 experiment carried out at the BM29 station.

---

This research has been carried out within the NUME Project “Development of composite proton membranes and of innovative electrode configurations for polymer electrolyte fuel cells” (MIUR, FISR 2003).

### References

- [1] V. R. Stamenkovic, et al. 2007 *Nature* **315** 493
- [2] S. Chen, et al. 2009 *J. Phys. Chem. C* **113** 1109
- [3] H. A. Gasteiger, et al. 2005 *Appl. Cat. B* **56** 9
- [4] Wlodarczyk R, et al. 2006 *J. Power Sources* **159** 802–809
- [5] Zurowski A 2008 *Cesium and rubidium salts of Keggin-type heteropolyacids as stable meso-microporous matrix for anode catalyst for H<sub>2</sub>/O<sub>2</sub> Proton Exchange Membrane Fuel Cell, Direct Methanol Fuel Cell and Direct Ethanol Fuel Cell*, PhD Thesis, Camerino University, Italy
- [6] Koningsberger D and Prins R 1988 *X-ray Absorption: Principles, Applications, Techniques of EXAFS, SEXAFS and XANES*, New York: Wiley-Interscience
- [7] Filippini A, Di Cicco A and Natoli C R 1995 *Phys. Rev.* **B 52** 15122–15134
- [8] Filippini A and Di Cicco A 1995 *Phys. Rev.* **B 52** 15135–15149
- [9] Witkowska A, Di Cicco A and Principi E 2007 *Phys. Rev. B* **76** 104110 (12 pages)

## Modelling of liquid crystalline polymers with anomalous mechanical properties

Ch. Zerafa<sup>1</sup>, M. R. Dudek<sup>2</sup>, A. C. Griffin<sup>3</sup>, K. W. Wojciechowski<sup>4</sup>,  
J. N. Grima<sup>1,5</sup>

<sup>1</sup>*Department of Chemistry, Faculty of Science, University of Malta  
Msida MSD2080, Malta*

<sup>2</sup>*Institute of Physics, Zielona Góra University  
65-069 Zielona Góra, Poland*

<sup>3</sup>*School of Materials Science and Engineering, Georgia Institute of Technology  
801 Ferst Drive, Atlanta, GA 30332-0295 USA*

<sup>4</sup>*Institute of Molecular Physics, Polish Academy of Sciences  
Smoluchowskiego 17, 60-179 Poznań, Poland*

<sup>5</sup>*Metamaterials Unit, Faculty of Science, University of Malta  
Msida MSD2080, Malta*

Recent research has led to the prediction, discovery and/or synthesis of various materials which exhibit negative Poisson's ratio. In particular, considerable advances have been made by Griffin et al. to synthesise nematic liquid crystalline polymers (LCPs) designed to exhibit this anomalous property [1–3]. This behaviour arises as a result of a mechanism involving re-orientation of laterally attached rod-like units, which in the unstressed state are aligned in the direction of the main polymer chain whilst in the stressed state they rotate to the orthogonal direction thus resulting in a lateral expansion when the polymer is stretched, as shown in Fig. 1a.

Force-field based molecular modelling simulations were performed using Accelrys Materials Studio v. 6.0 on polymeric systems based on Griffin's LCPs in an attempt to understand better the behaviour of these systems when they are stretched. Systems of various sizes were studied, where each unit cell contained from 4 up to 256 monomers, shown in Fig. 1b, in different systems (with a  $2 \times 2 \times 1$  and  $8 \times 8 \times 4$  configuration, respectively). The starting structure was optimised in such a way as to give a highly packed dense system. This was achieved by reducing the unit cell size to obtain extreme density, after which the system went back to a lower density following geometry optimisation. This system thus can be seen as representing (within the simulation error) the density close to the highest density possible at zero external pressure.

A strain was applied for several (up to 45) steps along the direction of the main chain (the Z-direction) by increasing the length of cell (parameter  $c$ ) by 1.75% in each single step, which was kept constant while the energy of the structure was minimised using the PCFF force-field [4]. External pressure was zero throughout the simulations, an approximation which is accounted for by the fact that atmospheric pressure is negligible with respect to the stress tensor corresponding to the strain applied.

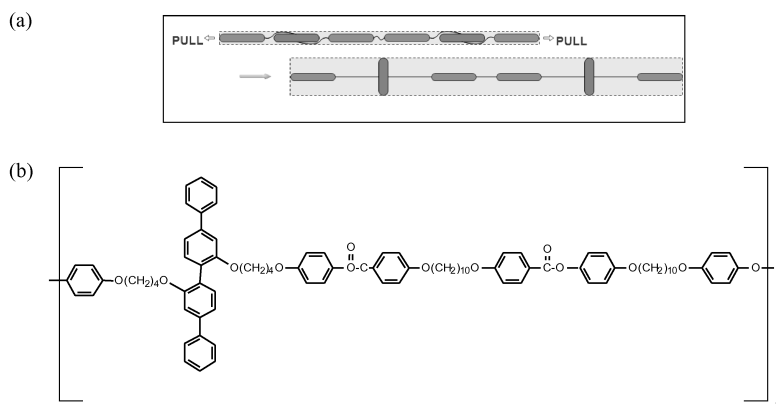


Figure 1: (a) The idea of nematic polymers showing auxetic behaviour; (b) The molecule studied.

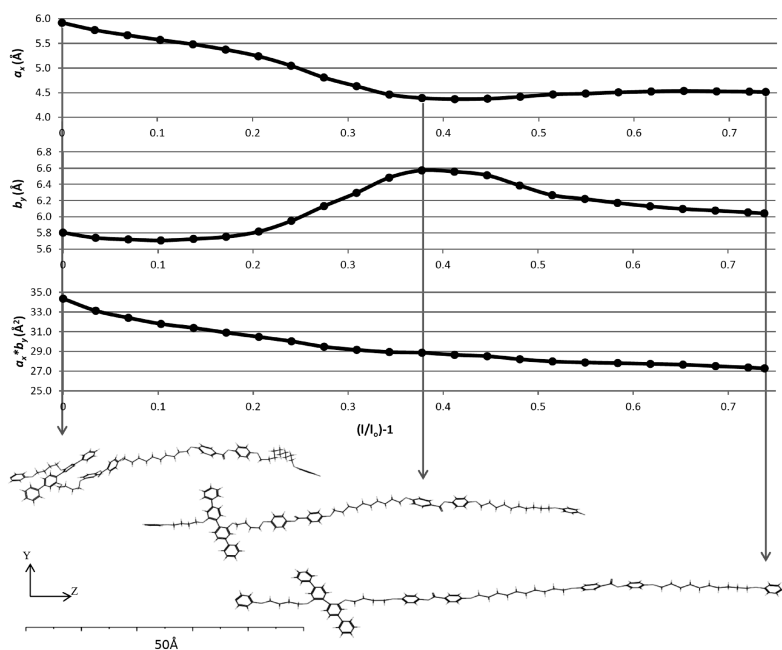


Figure 2: Dependence of the parameters  $a_x$ ,  $b_y$ , and the cross section area  $a_x b_y$  on the 'strain' (excess relative length) of the sample,  $l/l_0 - 1$ , for one of the studied systems (containing 256 monomers in an  $8 \times 8 \times 4$  configuration).

The calculations suggest that Poisson's ratio is clearly negative in the  $b_y$  direction and positive in the  $a_x$  direction, whilst the transverse area seems to decrease with increasing strain (see Fig. 2). The simulations show that the system is anisotropic in a direction transverse to the director of the nematic phase and it is necessary to

investigate larger systems (which are currently under study) in order to understand whether this effect survives in the bulk nematic phase.

Complimenting these simulations, theoretical modelling by analytic studies and computer simulation of a simplified (geometric) model are also being performed.

### **Acknowledgements**

This research is funded by a grant awarded to Christine Zerafa through the Strategic Educational Pathways Scholarship (Malta). These scholarships are part-financed by the European Union – European Social Fund (ESF) under Operational Programme II – Cohesion Policy 2007-2013, “Empowering People for More Jobs and a Better Quality of Life”. She is grateful to authorities of the Institute of Molecular Physics, Polish Academy of Sciences (IFM PAN), to members of the Division of Soft Matter Physics and Functional Materials, and the Department of Ferroelectrics for their hospitality at IFM PAN. She is also grateful for hospitality at the Institute of Physics, University of Zielona Góra. This research has been carried out using computational facilities procured through the European Regional Development Fund, Project ERDF-080 ‘A Supercomputing Laboratory for the University of Malta’ ([http://www.um.edu.mt/research/scienceeng/erdf\\_080](http://www.um.edu.mt/research/scienceeng/erdf_080)). Part of the simulations was performed at the Poznań Supercomputing and Networking Center.

### **References**

- [1] C. He, P. Liu, A. C. Griffin, *Macromolecules*, 31 (1998) 3145–3147
- [2] C. He, P. Liu, P. J. McMullan, A. C. Griffin, *Phys. Stat. Sol. B*, 242 (2004) 576–584.
- [3] C. He, P. Liu, A. C. Griffin, C. W. Smith, K. E. Evans, *Macromol. Chem. Phys.*, 206 (2005) 233–239.
- [4] H. Sun, S. Mumby, J. Maple, A. Hagler, *J. Am. Chem. Soc.*, 116 (1994) 2978.

---

## FMR study of influence of nitriding process of promoted nanocrystalline iron and nitrides reduction process at various nitriding potentials

G. Żołnierkiewicz<sup>1</sup>, N. Gouskos<sup>1,2</sup>, J. Typek<sup>1</sup>,  
A. Hełminiak<sup>3</sup>, W. Arabczyk<sup>3</sup>

<sup>1</sup>*Institute of Physics, West Pomeranian University of Technology  
Al Piastow 48, 70-311, Poland*

<sup>2</sup>*Department of Solid State Physics, Faculty of Physics, University of Athens  
Panepistimiopolis, 15 784 Zografou, Athens, Greece*

<sup>3</sup>*Institute of Chemical and Environmental Engineering  
West Pomeranian University of Technology  
Al. Piastow 17, 70-311, Poland*

The effects of the nitriding process of promoted nanocrystalline iron and the nitride reduction process at the various nitriding potentials (P) on the thermodynamic parameters were investigated. During the studied processes two parallel reactions occurred:

- the nitriding reaction, penetration of chemisorbed atomic nitrogen to the crystallographic space in the lattice system of iron ( $\alpha$ -Fe(N)), phase transition to iron nitride  $\gamma$ '-Fe<sub>4</sub>N and next, to  $\varepsilon$ -Fe<sub>x</sub>N were observed when a critical bulk concentration of nitrogen was reached;
- the surface reaction of catalytic ammonia decomposition.

The gas nitriding and reduction were studied in a differential reactor equipped with systems that made it possible to conduct both thermogravimetric measurements ( $\alpha_{Fe}$ ) and hydrogen concentration analyses in the reacting gas mixture. The nitriding and reduction processes were investigated under ammonia–hydrogen mixtures (various P), under atmospheric pressure, at 400°C and 475°C. It was found that stationary states existed during the nitriding process as well as the reduction process, wherein it was only the catalytic ammonia decomposition reaction that was occurring. The hysteresis phenomenon occurred in the system: nitriding of nanocrystalline iron and reduction of nanocrystalline nitrides for  $\alpha_{Fe} = f(\ln P)$ . Ferromagnetic resonance (FMR) spectra of Fe<sub>x</sub>N and  $\alpha$ -Fe nanoparticles were recorded at room temperature in the samples subjected to different nitriding processes. The FMR spectra obtained at room temperature showed essential differences between them and were analyzed in terms of four components having the Callen lineshape. They revealed the existence of an anisotropic magnetic interaction in two types of nanoparticles. The anisotropic resonance fields (parallel and perpendicular) were used to determine the magnitude of

the anisotropy fields for both types of nanoparticles while the dipol-dipol interaction between nanoparticles was responsible for the linewidths of the spectral components. The observed behavior was different than in a previously prepared system [1].

**References**

- [1] A. Helminiak, W. Arabczyk, G. Zolnierkiewicz, N. Guskos, and J. Typek, *Rev. Adv. Mat. Sci.* **29**, 166 (2011)

## The 55<sup>th</sup> birthday of Sergei Kruchinin



In 2012, the famous physicist-theorist, Professor Sergei Pavlovich Kruchinin, Ph. D. in Phys.-Math. Sci., a leading scientific researcher of the N. N. Bogolyubov Institute for Theoretical Physics of the NAS of Ukraine, Head of the Chair of Applied Physics at the National Aviation University, celebrates his 55<sup>th</sup>, birthday.

S. P. Kruchinin was born on February 6, 1957 in the town of Krasnyi Luch in the Lugansk region. In 1979, he graduated from the Physical Faculty of the T. G. Shevchenko Kiev State University and started his post-graduate course at the Chair of Theoretical Physics in Kiev under the guidance of Professor G. F. Filippov who developed the theory of nonaxial nuclei jointly with A. S. Davydov, Academician of the NAS of Ukraine. Having defended his Candidate degree thesis entitled *Coupling of Collective and Internal Degrees of Freedom in Few-Nucleon Systems* in 1986, Sergei Pavlovich was invited by A. S. Davydov to work in his group. Since that time, the scientific and scientific-organizational activities of Sergei Pavlovich have been closely connected with A. S. Davydov and the Institute for Theoretical Physics.

In 2002, S. P. Kruchinin defended his Ph. D. thesis entitled *Thermodynamical Effects in High-Temperature Superconductors* in the major of *Theoretical and Mathematical Physics*.

S. P. Kruchinin has published significant original works in the fields of nuclear physics and many-particle systems, solid-state physics, superconductivity, theory of nonlinear phenomena, nanophysics.

S. P. Kruchinin is the author and co-author of more than 80 scientific works which have been published in leading scientific journals. He has been using advanced mathematical methods to solve the posed problems.

In the article *On the Nature of Resonances Observed in Photonuclear Reactions* (*Nuclear Physics* (1986), S. P. Kruchinin, jointly with G. F. Filippov), the coupling of collective and cluster degrees of freedom in light nuclei was studied, and the nature of resonances in photo-nuclear reactions observed in experiments was explained.

Since the time high-temperature superconductors were discovered, S. P. Kruchinin has intensively studied their physical properties.

In particular, it is worth noting the work carried out jointly with A. S. Davydov *Interlayer Effects in the Newest High- $T_c$  Superconductors* (*Physica C*, 1991), where the theory of the nonmonotonous dependence of the critical temperature of superconductivity on the number of cuprate layers in the elementary cell of high-temperature superconductors was developed.

This work has remained up to date in connection with the search for new superconductors operating at room temperature.

The investigation of high-temperature superconductivity mechanisms is one of the priority directions of the studies to which Sergei Pavlovich has been paying much attention.

In the work *Functional Integral of Antiferromagnetic Spin Fluctuations in High-Temperature Superconductors* (*Modern Phys. Letters B*, 1995), S. P. Kruchinin proposed a continual model of a spin-fluctuation mechanism for high-temperature superconductors and calculated the thermodynamic properties of superconductors with  $d$ -pairing.

The experimental discovery of superconductivity in magnesium diborides stimulated a new stage of studies for Sergei Pavlovich such as the development of a multi-band model of superconductivity. In this field, one of the works by S. P. Kruchinin jointly with H. Nagao, namely *Multiband Superconductivity in Int. J. Mod. Phys.* (2002), should be mentioned.

Kruchinin's works on superconductivity were included in the monograph *Modern aspects of Superconductivity: Theory of Superconductivity* (*World Scientific*, Singapore, 2010, jointly with H. Nagao) which shows the contemporary status of the problems of high-temperature superconductivity.

In the last years, S. P. Kruchinin has been working intensively in the theory of nanosystems and new materials. The important work performed jointly with N. N. Bogolyubov (jr.) Corresponding Member of the Russian Academy of Sciences, *Method of Intermediate Problems in the Theory of Gaussian Dots Placed in a Magnetic Field* (*Condensed Matter Physics*, 2006) should be noted, where the spectrum and eigenfunctions of a system of quantum dots with the Gauss interaction in a magnetic field were calculated. It was shown that such systems were of significant importance for nanotechnologies.

A number of works by S. P. Kruchinin are devoted to hybrid "superconductor-ferromagnetic" nanosystems. In the article *Interactions of Nanoscale Ferromagnetic Granules in a London Superconductor* (*Supercond. Sci. Technol.* (2006), jointly with J. Annett), the interaction of ferromagnetic granules in a London superconductor is studied, and it is shown that such a system is characterized by temperature-dependent spin-orientation phase transitions.

It is also the works on the theory of nanotransistors, quantum computers, and composites with radioactive inclusions which were published in the last years that are worth noting.

S. P. Kruchinin has found much time to train scientific personnel. He is the Head of the Chair of Applied Physics at the National Aviation University (Kyiv).

This chair was established by A. P. Shpak, Academician of the NAS of Ukraine in 2002. Its main scientific trends have been the physics of nanosystems and the physics of modern energy systems.

Sergei Pavlovich was the organizer of six international conferences on the current problems of high-temperature superconductivity and nanosystems which were held in the town of Yalta. These conferences promoted the development of international cooperation, including Russia and Ukraine. Five books in *Springer* and one book in *World Scientific* publishing houses were published under his guidance.

S. P. Kruchinin was the leader of many international projects supported by the Ministry of Education and Science of Ukraine, INTAS, CRDF (USA), Royal Society (Great Britain), DFG (Germany), JSPS (Japan), etc.

S. P. Kruchinin is Academician of the International Academy of Creation (Russia, 2007), member of the New York Academy of Sciences (USA, 1998), and member of the International Association of Mathematical Physics (France, 1996).

The scientific community and colleagues cordially congratulate Sergei Pavlovich on this significant occasion and wish him good health and many new creative achievements.

# INDEX OF AUTHORS

- Alderson, A., 28  
Alderson, K. L., 28  
Amirabadizadeh, A., 59  
Ania, F., 14  
Annett, J. F., 13  
Arabczyk, W., 103  
Attard, D., 25, 66, 80  
Azzopardi, K. M., 66  
Baltá-Calleja, F. J., 14  
Belomestnykh, V., 16  
Berczyński, P., 23, 73, 77  
Białoskórski, M., 60  
Bletsa, E., 62  
Bojarska, A., 87  
Borucka-Lipska, J., 24  
Butwin, A., 18  
Camilleri, M., 25  
Caruana-Gauci, R., 25, 63, 64  
Casha, A., 25, 80  
Cauchi, R., 25, 66  
Chetcuti, E., 25  
Cicco, A. Di, 98  
Cutajar, J. D., 25  
Czech, Z., 18  
Dawid, A., 67  
Deligiannakis, Y., 62  
Dendzik, Z., 69  
Dolat, D., 23  
Drzewiecki, A., 39, 90  
Dsoke, S., 98  
Duan, X.-M., 19  
Dudek, K., 80  
Dudek, M. R., 53, 63, 100  
Ellul, B., 25  
Flores, A., 14  
Gatt, R., 25, 66, 80  
Gburski, Z., 21, 67, 69, 94  
Giannakopoulou, T., 42, 50  
Giannouri, M., 50  
Glenis, S., 73, 77  
Godlewski, M., 30  
Goldstein, R. V., 70  
Gorodtsov, V. A., 70  
Gournis, D., 22, 55, 62  
Gouskos, N., 23, 24, 30, 42, 51, 53,  
73, 74, 76, 77, 79, 91, 103  
Górny, K., 21, 67, 69  
Griffin, A. C., 46, 100  
Grima, J. N., 25, 63, 64, 66, 80, 100  
Grinberg, M., 26  
Grzmił, B., 23  
Guskos, A., 23, 24, 73, 76, 77  
Hadjiagapiou, I., 27  
Hełminiak, A., 103  
Hewage, T. A. M., 28

Imre, A. R., 29  
 Jaworski, S., 49  
 Kajak, P., 81  
 Kaszewski, J., 30  
 Kempniński, M., 32  
Kempniński, W., 32  
Kędziora, P., 82  
 Kiernożycki, W., 24  
 Kline, W., 46  
 Kopayev, A. V., 39  
Kościelska, B., 83  
 Kouloumpis, A., 55  
 Kowalik, M., 88  
 Kozioł, J. J., 53  
 Kościelska, B., 87  
Kruchinin, S. P., 13, 84  
 Krupska, A., 74  
 Kulyk, Yu. O., 90  
 Kusiak, E., 30  
Kwiatkowska, M., 33, 85  
Kwiatkowski, K., 33, 85  
 Lendzion-Bieluń, Z., 73  
Lipiński, I. E., 86  
 Lisiecki, R., 91  
Lisovenko, D. S., 70  
Łapiński, M., 87  
 Łojkowski, W., 73  
 Łoś, Sz., 32  
 Łukaszczuk, P., 30  
 Majszczyk, J., 76  
 Manicaro, E., 25  
 Marassi, R., 98  
 Markowski, D., 32  
 McMullan, P. J., 46  
 Mijowska, E., 30  
 Mizzi, L., 25  
Morawski, A., 23  
 Morawski, W., 30  
 Mudry, S. I., 90  
Narkiewicz, U., 30, 73, 79  
Narojczyk, J. W., 88  
Nawrocki, W., 35  
 Ołdziejewski, Ł., 49  
 Orlikowski, J., 30  
 Pabiszczak, M., 21, 94  
Padlyak, B. V., 39, 53, 90, 91  
Papadopoulos, G. J., 41  
 Pelech, I., 30  
Peng, H. X., 44  
Petridis, D., 42, 50, 77  
Polanowski, P., 43  
Poźniak, A. A., 52, 93  
 Qin, F. X., 44  
Raczyński, P., 21, 94  
 Ren, W., 46  
 Rudolf, P., 55  
 Ryba-Romanowski, W., 91  
Rybicki, J., 60, 66, 76, 81, 97  
 Rysiakiewicz-Pasek, E., 53  
 Sadowski, W., 87  
Sarlis, N. V., 47  
 Sibera, D., 73, 76  
Sikorski, A., 49  
Soboleva, E., 16

Soboń, M., 86  
Sowa, D., 18  
Stathi, P., 55  
Tafiychuk, Yu. N., 39  
Todorova, N., 42, 50  
Trapalis, C., 42, 50  
Tretiakov, K. V., 95  
Tsoufis, T., 55  
Typek, J., 23, 24, 51, 73, 74, 76, 79, 103  
Vermisoglou, E. C., 42, 50  
Wardal, K., 51, 73  
Wicikowski, L., 83  
Winczewski, S., 97  
Witkowska, A., 83, 98  
Wojciechowski, K. W., 52, 63, 64,  
88, 93, 95, 100  
Wolak, W., 80  
Yatsunenko, S., 30  
Zadnieprianniy, D. L., 39  
Zapotoczny, B., 53  
Zerafa, Ch., 25, 100  
Zolotovskiy, A. A., 13, 84  
Zygouri, P., 55  
Żołnierkiewicz, G., 23, 24, 30, 51,  
73, 79, 91, 103